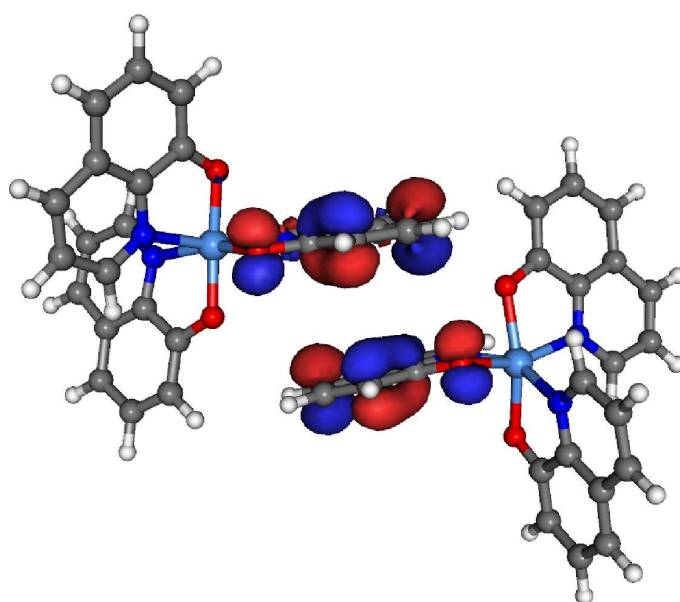


VOTCA-CTP

CHARGE TRANSPORT SIMULATIONS

USER MANUAL



compiled from: 1.5 ()

January 28, 2019

www.votca.org

Disclaimer

Open source projects are made available and contributed to under licenses that include terms that, for the protection of contributors, make clear that the projects are offered “as-is”, without warranty, and disclaiming liability for damages resulting from using the projects.

Citations

Development of this software depends on academic research grants. If you are using the package, please cite the following papers

[1] Long-range embedding of molecular ions and excitations in a polarizable molecular environment, Carl Poelking and Denis Andrienko
J. Chem. Theory Comp. 12, 4516, 2016

[2] Modeling of spatially correlated energetic disorder in organic semiconductors, Pascal Kordt, Denis Andrienko
J. Chem. Theory Comput., 12, 36, 2016

[3] Microscopic simulations of charge transport in disordered organic semiconductors, Victor Rühle, Alexander Lukyanov, Falk May, Manuel Schrader, Thorsten Vehoff, James Kirkpatrick, Björn Baumeier and Denis Andrienko
J. Chem. Theor. Comp. 7, 3335, 2011

[4] Extracting nondispersive charge carrier mobilities of organic semiconductors from simulations of small systems, A. Lukyanov, D. Andrienko
Phys. Rev. B, 82, 193202, 2010

[5] Density-functional based determination of intermolecular charge transfer properties for large-scale morphologies, Björn Baumeier, James Kirkpatrick, and Denis Andrienko
Phys. Chem. Chem. Phys. 12, 11103, 2010

[6] Versatile Object-oriented Toolkit for Coarse-graining Applications, Victor Rühle, Christoph Junghans, Alexander Lukyanov, Kurt Kremer and Denis Andrienko
J. Chem. Theor. Comp. 5, 3211, 2009

[7] An approximate method for calculating transfer integrals based on the ZINDO Hamiltonian, James Kirkpatrick,
Int. J. Quantum Chem. 108, 51, 2007

Copyright

VOTCA-CTP is free software. The entire package is available under the Apache License. For details, check the LICENSE file in the source code. The VOTCA-CTP source code is available on our homepage, www.votca.org.

Contents

1	Introduction	3
2	Theoretical background	5
2.1	Workflow	5
2.2	Material morphology	5
2.3	Conjugated segments and rigid fragments	6
2.4	Neighbor list	8
2.5	Reorganization energy	8
2.5.1	Intramolecular reorganization energy	8
2.5.2	Outersphere reorganization energy	9
2.6	Site energies	10
2.6.1	Externally applied electric field	10
2.6.2	Internal energy	11
2.6.3	Electrostatic interaction energy	11
2.6.4	Induction energy - the Thole model	12
2.6.5	Long-range Coulomb interactions	14
2.7	Transfer integrals	19
2.7.1	Projection of monomer orbitals on dimer orbitals (DIPRO)	19
2.7.2	DFT-based transfer integrals using DIPRO	20
2.7.3	ZINDO-based transfer integrals using MOO	23
2.8	Charge transfer rate	24
2.8.1	Classical charge transfer rate	24
2.8.2	Semi-classical bimolecular rate	24
2.8.3	Semi-classical rate	25
2.9	Master equation	25
2.9.1	Extrapolation to nondispersive mobilities	26
2.10	Macroscopic observables	26
2.10.1	Charge density	27
2.10.2	Current	27
2.10.3	Mobility and diffusion constant	27
2.10.4	Spatial correlations of energetic disorder	28
2.10.5	DFT-based transfer integrals using DIPRO	28
3	Input and output files	31
3.1	Atomistic topology	31
3.2	Mapping file	33
3.3	Conjugated segments	34
3.4	Molecular orbitals	35
3.5	Monomer calculations for DFT transfer integrals	36
3.6	Pair calculations for DFT transfer integrals	37
3.7	DFT transfer integrals	39
3.8	State file	40

4 Reference	43
4.1 Programs	43
4.1.1 ctp_map	43
4.1.2 ctp_dump	43
4.1.3 ctp_tools	43
4.1.4 ctp_run	44
4.1.5 ctp_parallel	44
4.1.6 moo_overlap	44
4.2 Calculators	45
4.2.1 coupling	45
4.2.2 log2mps	46
4.2.3 molpol	46
4.2.4 pdb2map	46
4.2.5 pdb2top	46
4.2.6 ptopreader	47
4.2.7 eanalyze	47
4.2.8 eimport	47
4.2.9 einternal	47
4.2.10 emultipole	47
4.2.11 eoutersphere	48
4.2.12 ewdbgpol	49
4.2.13 ianalyze	49
4.2.14 iimport	49
4.2.15 izindo	49
4.2.16 jobwriter	49
4.2.17 neighborlist	50
4.2.18 pairedump	50
4.2.19 profile	50
4.2.20 rates	50
4.2.21 sandbox	51
4.2.22 stateserver	51
4.2.23 tdump	51
4.2.24 vaverage	51
4.2.25 zmultipole	52
4.2.26 edft	52
4.2.27 idft	53
4.2.28 pewald3d	53
4.2.29 qmmm	53
4.2.30 xqmultipole	54
4.2.31 energy2xml	55
4.2.32 integrals2xml	55
4.2.33 occupations2xml	55
4.2.34 pairs2xml	55
4.2.35 rates2xml	56
4.2.36 segments2xml	56
4.2.37 trajectory2pdb	56
Bibliography	57

Index

- charge transfer rate, 22
 - bimolecular, 22
 - classical, 22
 - semiclassical, 23
- conjugated segment, 4
- current, 25
 - local, 25
- diabatic states, 17
- distributed multipoles, 9
- electronic coupling, 17
 - DFT, 18, 26
 - ZINDO, 21
- hopping site, 4
- kinetic Monte Carlo, 23
- Long-range interactions, 12
- mobility, 25
- neighbor list, 6
- Pekar factor, 8
- reorganization energy, 6
 - intramolecular, 6
 - outersphere, 7
- rigid fragment, 5
- site energy, 8
 - distributed multipoles, 9
 - Ewald, 12
 - external field, 8
 - internal, 9
 - polarization, 10
 - spatial correlation, 26
- Thole model, 10
- transfer integral, *see* electronic coupling

Chapter 1

Introduction

sec:introduction

Charge carrier dynamics in an organic semiconductor can often be described in terms of charge hopping between localized states. The hopping rates depend on **electronic coupling elements**, **reorganization energies**, and **site energies**, which vary as a function of position and orientation of the molecules. The purpose of the VOTCA-CTP package [3] is to simplify the workflow for charge transport simulations, provide a uniform error-control for the methods, flexible platform for their development, and eventually allow *in silico* prescreening of organic semiconductors for specific applications.

The toolkit is implemented using modular concepts introduced earlier in the Versatile Object-oriented Toolkit for Coarse-graining Applications (VOTCA) [6]. It contains different **programs**, which execute specific tasks implemented in **calculators** representing an individual step in the workflow. Figure 1.1 summarizes a typical chain of commands to perform a charge transport simulation: First, the VOTCA code structures are adapted to reading atomistic trajectories, mapping them onto conjugated segments and rigid fragments, and substituting (if needed) rigid fragments with the optimized copies (`ctp_map`). The programs `ctp_run` and `ctp_parallel` (for heavy-duty tasks) are then used to calculate all bimolecular charge hopping rates (via precalculation of all required ingredients). **Site energies (or energetic disorder)** can be determined as a combination of internal (ionization potentials/electron affinities of single molecules) as well as electrostatic and polarization contributions within the molecular environment. The calculation of **electronic coupling elements** between conjugated segments from the corresponding molecular orbitals can be performed using a **dimer-projection** technique based on **density-functional** theory (DFT). This requires explicit calculations using quantum-chemistry software for which we provide interfaces to `Gaussian`, `Turbomole`, and `NWChem`. Alternatively, the **molecular orbital overlap** module calculates electronic coupling elements relying on the semi-empirical INDO Hamiltonian and molecular orbitals in the format provided by the `Gaussian` package.

The **kinetic Monte Carlo** module reads in the neighbor list, site coordinates, and hopping rates and performs charge dynamics simulations using either periodic boundary conditions or charge sources and sinks.

The toolkit is written as a combination of modular C++ code and scripts. The data transfer between programs is implemented via a state file (sql database), which is also used to restart simulations. Analysis functions and most of the calculation routines are encapsulated by using the observer pattern [8] which allows the implementation of new functions as individual modules.

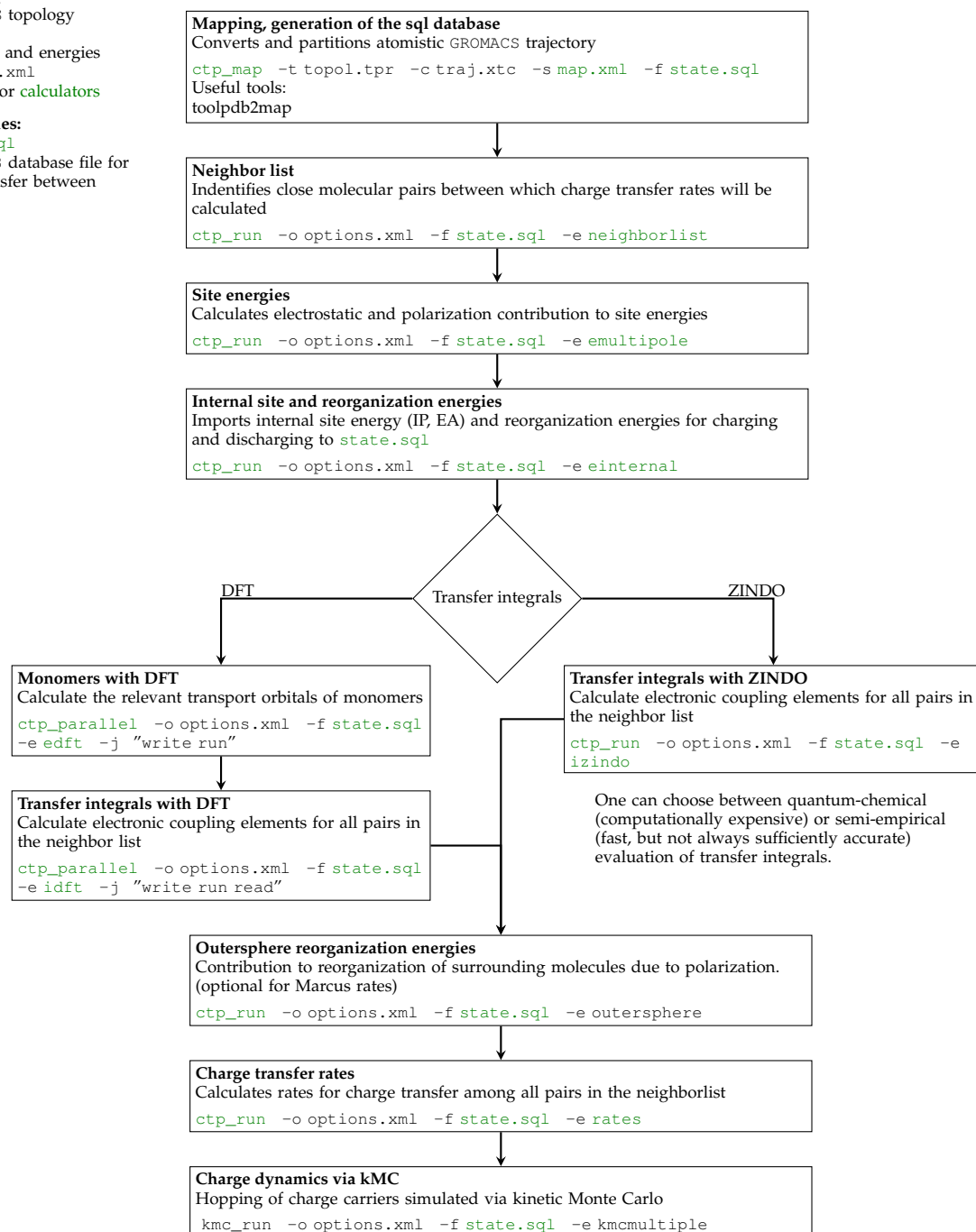
In the following chapter 2, we summarize the **theoretical background** of the workflow of charge transport simulations and in particular its individual steps. Chapter 3 describes the structure and content of input and output files, while a full reference of **programs** and **calculators** is available in chapter 4. For a hands-on tutorial, the reader is referred to the VOTCA-CTP project page at <http://code.google.com/p/votca-ctp/>.

Input files:

conf.gro
 GROMACS trajectory
 topol.tpr
 GROMACS topology
 map.xml
 mapping and energies
 options.xml
 options for **calculators**

Output files:

state.sql
 sqlite3 database file for
 data transfer between
 modules



Get list of available calculators: `ctp_run/ctp_parallel/kmc_run -l`

Get help and list of options for a calculator: `ctp_run/ctp_parallel/kmc_run -d neighborlist`

Figure 1.1: A practical workflow of charge transport simulations using VOTCA-CTP. The **theoretical background** of the individual steps is given in chapter 2. Chapter 3 describes the content of input and output files, while a full reference of **programs** and **calculators** is available in chapter 4. [fig:summary](#)

Chapter 2

Theoretical background

2.1 Workflow

A typical workflow of charge transport simulations is depicted in figure 2.1. The first step is the simulation of an atomistic morphology, which is then partitioned on hopping sites. The coordinates of the hopping sites are used to construct a list of pairs of molecules, or neighbor list.

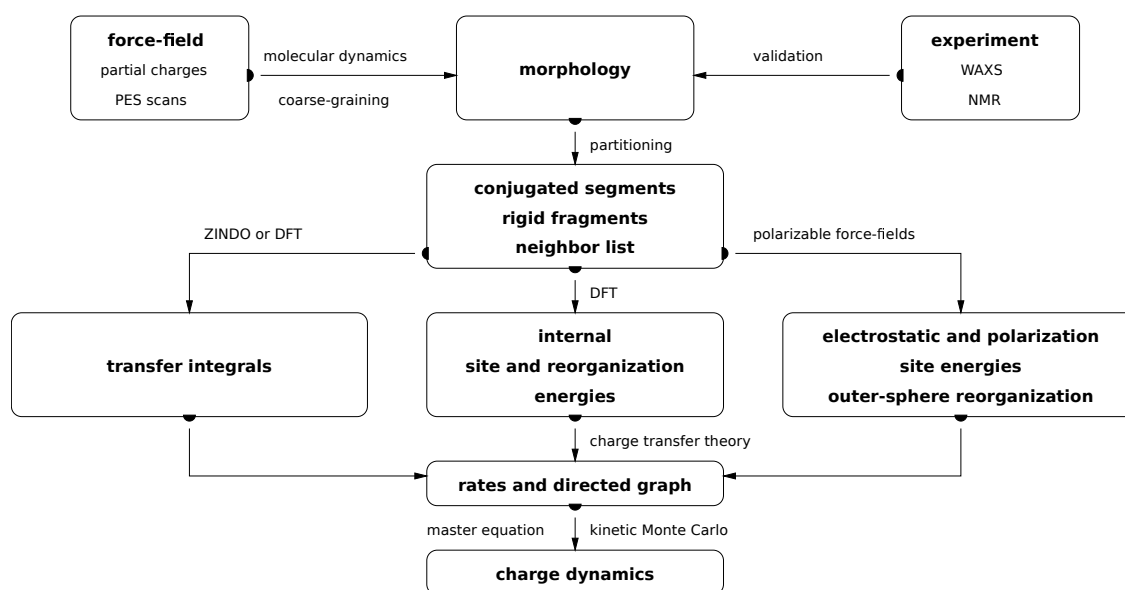


Figure 2.1: Workflow for microscopic simulations of charge transport.

For each pair an electronic coupling element, a reorganization energy, a driving force, and eventually the hopping rate are evaluated. The neighbor list and hopping rates define a directed graph. The corresponding master equation is solved using the kinetic Monte Carlo method, which allows to explicitly monitor the charge dynamics in the system as well as to calculate time or ensemble averages of occupation probabilities, charge fluxes, correlation functions, and field-dependent mobilities.

2.2 Material morphology

There is no generic recipe on how to predict a large-scale atomistically-resolved morphology of an organic semiconductor. The required methods are system-specific: for ultra-pure crystals, for

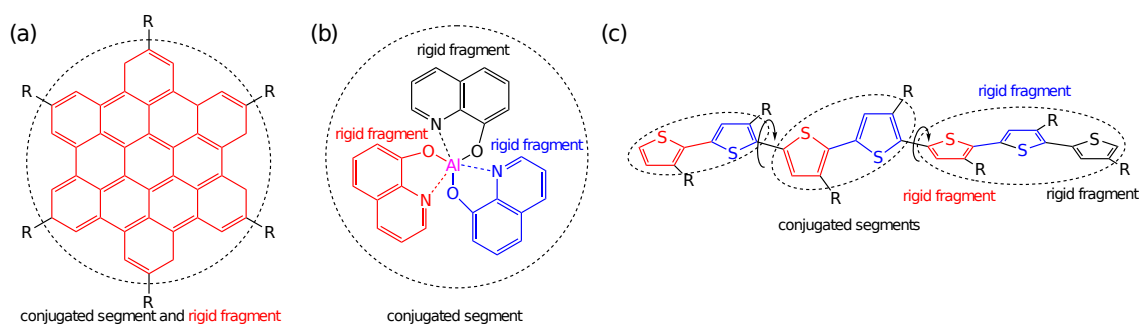


Figure 2.2: The concept of conjugated segments and rigid fragments. Dashed lines indicate conjugated segments while colors denote rigid fragments. (a) Hexabenzocoronene: the π -conjugated system is both a rigid fragment and a conjugated segment. (b) Alq₃: the Al atom and each ligand are rigid fragments while the whole molecule is a conjugated segment. (c) Polythiophene: each repeat unit is a rigid fragment. A conjugated segment consists of one or more rigid fragments. One molecule can have several conjugated segments.

fig:segment

54 example, density-functional methods can be used provided the crystal structure is known from
 55 experiment. For partially disordered organic semiconductors, however, system sizes much larger
 56 than a unit cell are required. Classical molecular dynamics or Monte Carlo techniques are then
 57 the methods of choice.

58 In molecular dynamics, atoms are represented by point masses which interact via empirical po-
 59 tentials prescribed by a force-field. Force-fields are parametrized for a limited set of compounds
 60 and their refinement is often required for new molecules. In particular, special attention shall
 61 be paid to torsion potentials between successive repeat units of conjugated polymers or between
 62 functional groups and the π -conjugated system. First-principles methods can be used to charac-
 63 terize the missing terms of the potential energy function.

64 Self-assembling materials, such as soluble oligomers, discotic liquid crystals, block copolymers,
 65 partially crystalline polymers, etc., are the most complicated to study. The morphology of such
 66 systems often has several characteristic length scales and can be kinetically arrested in a thermo-
 67 dynamically non-equilibrium state. For such systems, the time- and length-scales of atomistic
 68 simulations might be insufficient to equilibrate or sample desired morphologies. In this case,
 69 systematic coarse-graining can be used to enhance sampling [6]. Note that the coarse-grained
 70 representation must reflect the structure of the atomistic system and allow for back-mapping to
 71 the atomistic resolution.

72 Here we assume that the morphology is already known, that is we know how the topology and
 73 the coordinates of all atoms in the systems at a given time. VOTCA-CTP can read standard
 74 GROMACS topology files. Custom definitions of **atomistic topology** via XML files are also possible.
 75 Since the description of the atomistic topology is the first step in the charge transport simulations,
 76 it is important to follow simple conventions on how the system is partitioned on molecules,
 77 residues, and how atoms are named in the topology. Required input files are described in section
 78 **atomistic topology**.

79 2.3 Conjugated segments and rigid fragments

sec:segments

80 With the morphology at hand, the next step is partitioning the system on hopping sites, or con-
 81 jugated segments, and calculating charge transfer rates between them. Physically intuitive argu-
 82 ments can be used for the partitioning, which reflects the localization of the wave function of
 83 a charge. For most organic semiconductors, the molecular architecture includes relatively rigid,
 84 planar π -conjugated systems, which we will refer to as rigid fragments. A conjugated segment
 85 can contain one or more of such rigid fragments, which are linked by bonded degrees of freedom.

86 The dynamics of these degrees of freedom evolves on timescales much slower than the frequency
 87 of the internal promoting mode. In some cases, e.g. glasses, it can be ‘frozen’ due to non-bonded
 88 interactions with the surrounding molecules.

89 To illustrate the concept of conjugated segments and rigid fragments, three representative molec-
 90 ular architectures are shown in figure 2.2. The first one is a typical discotic liquid crystal, hex-
 91 abenzocoronene. It consists of a conjugated core to which side chains are attached to aid self-
 92 assembly and solution processing. In this case the orbitals localized on side chains do not partic-
 93 ipate in charge transport and the conjugated π -system is both, a rigid fragment and a conjugated
 94 segment. In Alq_3 , a metal-coordinated compound, a charge carrier is delocalized over all three
 95 ligands. Hence, the whole molecule is one conjugated segment. Individual ligands are relatively
 96 rigid, while energies of the order of $k_B T$ are sufficient to reorient them with respect to each other.
 97 Thus the Al atom and the three ligands are rigid fragments. In the case of a conjugated polymer,
 98 one molecule can consist of several conjugated segments, while each backbone repeat unit is a
 99 rigid fragment. Since the conjugation along the backbone can be broken due to large out-of-plane
 100 twists between two repeat units, an empirical criterion, based on the dihedral angle, can be used
 101 to partition the backbone on conjugated segments [9]. However, such intuitive partitioning is, to
 102 some extent, arbitrary and shall be validated by other methods [10–12].

103 After partitioning, an additional step is often required to remove bond length fluctuations intro-
 104 duced by molecular dynamics simulations, since they are already integrated out in the deriva-
 105 tion of the rate expression. This is achieved by substituting respective molecular fragments with
 106 rigid, planar π -systems optimized using first-principles methods. Centers of mass and gyration
 107 tensors are used to align rigid fragments, though a custom definition of local axes is also possible.
 108 Such a procedure also minimizes discrepancies between the force-field and first-principles-based
 109 ground state geometries of conjugated segments, which might be important for calculations of
 110 electronic couplings, reorganization energies, and intramolecular driving forces.

111 To partition the system on hopping sites and substitute rigid fragments with the corresponding
 112 ground-state geometries `ctp_map` program is used:

Mapping the GROMACS trajectory

```
| ctp_map -t topol.tpr -c traj.xtc -s map.xml -f state.sql
```

113 It reads in the GROMACS topology (`topol.tpr`) and trajectory (`traj.xtc`) files, definitions of
 114 conjugated segments and rigid fragments (`map.xml`) and outputs coordinates of conjugated seg-
 115 ments (hopping sites) and rigid fragments (as provided in the MD trajectory and after rigidi-
 116 fication) to the state file (`state.sql`). In order to do this, a mapping file `map.xml` has to be
 117 provided, which specifies the corresponding atoms in the different representations. After this
 118 step, all information (frame number, dimensions of the simulation box, etc) are stored in the state
 119 file and only this file is used for further calculations.

Attention

| VOTCA-CTP requires a wrapped trajectory for mapping the segments and fragments, so all molecules
 should be whole in the frame.

120 In order to visually check the mapping one can use either the `t_dump` calculator or the programm
 121 `ctp_dump` with the calculator `trajectory2pdb`.

sec:ctp_dump

Writing a mapped trajectory with `ctp_dump`

```
| ctp_dump -f state.sql -e trajectory2pdb
```

122 It reads in the state file created by `ctp_map` and outputs two trajectory files corresponding to
 123 the original and rigidified atom coordinates. To check the mapping, it is useful to superimpose
 124 the three outputs (original atomistic, atomistic stored in the state file, and rigidified according to
 125 ground state geometries), e.g., with VMD.

sec:tdump

Writing a mapped trajectory with `tdump`

```
1 | ctp_run -f state.sql -o options.xml -e tdump
```

126 It also reads in the state file but appends the coordinates to a `pdb` file. So make sure to delete old
 127 `QM.pdb` and `MD.pdb` if you want to create a new imagef

128 2.4 Neighbor list

sec:neighborlist

129 A list of neighboring conjugated segments, or neighbor list, contains all pairs of conjugated seg-
 130 ments for which `coupling elements`, `reorganization energies`, `site energy differences`, and `rates`
 131 are evaluated.

132 Two segments are added to this list if the distance between centers of mass of any of their rigid
 133 fragments is below a certain cutoff. This allows neighbors to be selected on a criterion of min-
 134 imum distance of approach rather than center of mass distance, which is useful for molecules
 135 with anisotropic shapes.

136 The neighbor list can be generated from the atomistic trajectory by using the `neighborlist`
 137 `calculator`. This calculator requires a cutoff, which can be specified in the `options.xml` file. The
 138 list is saved to the `state.sql` file:

Generating a neighbor list

```
1 | ctp_run -o options.xml -f state.sql -e neighborlist
```

139 2.5 Reorganization energy

sec:reorganization

140 The reorganization energy λ_{ij} takes into account the change in nuclear (and dielectric) degrees of
 141 freedom as the charge moves from donor i to acceptor j . It has two contributions: intramolecular,
 142 $\lambda_{ij}^{\text{int}}$, which is due to reorganization of nuclear coordinates of the two molecules forming the
 143 charge transfer complex, and intermolecular (outersphere), $\lambda_{ij}^{\text{out}}$, which is due to the relaxation of
 144 the nuclear coordinates of the environment. In what follows we discuss how these contributions
 145 can be calculated.

146 2.5.1 Intramolecular reorganization energy

sec:intramolecular

147 If intramolecular vibrational modes of the two molecules are treated classically, the rearrange-
 148 ment of their nuclear coordinates after charge transfer results in the dissipation of the internal
 149 reorganization energy, $\lambda_{ij}^{\text{int}}$. It can be computed from four points on the potential energy surfaces
 150 (PES) of both molecules in neutral and charged states, as indicated in figure 2.3.

151 Adding the contributions due to discharging of molecule i and charging of molecule j yields [13]

$$\lambda_{ij}^{\text{int}} = \lambda_i^{cn} + \lambda_j^{nc} = U_i^{nC} - U_i^{nN} + U_j^{cN} - U_j^{cC}. \quad (2.1) \quad \text{equ:lambda}$$

152 Here U_i^{nC} is the internal energy of the neutral molecule i in the geometry of its charged state
 153 (small n denotes the state and capital C the geometry). Similarly, U_j^{cN} is the energy of the charged
 154 molecule j in the geometry of its neutral state. Note that the PES of the donor and acceptor are
 155 not identical for chemically different compounds or for conformers of the same molecule. In this

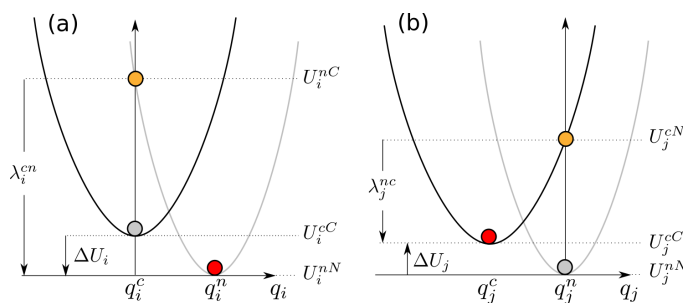


Figure 2.3: Potential energy surfaces of (a) donor and (b) acceptor in charged and neutral states. After the change of the charge state both molecules relax their nuclear coordinates. If all vibrational modes are treated classically, the total internal reorganization energy and the internal energy difference of the electron transfer reaction are $\lambda_{ij}^{\text{int}} = \lambda_i^{\text{cn}} + \lambda_j^{\text{nc}}$ and $\Delta E_{ij}^{\text{int}} = \Delta U_i - \Delta U_j$, respectively.

fig.parabolas

156 case $\lambda_i^{\text{cn}} \neq \lambda_j^{\text{cn}}$ and $\lambda_i^{\text{nc}} \neq \lambda_j^{\text{nc}}$. Thus $\lambda_{ij}^{\text{int}}$ is a property of the charge transfer complex, and not of
 157 a single molecule.

158 Intramolecular reorganization energies for discharging (λ^{cn}) and charging (λ^{nc}) of a molecule
 159 need to be determined using quantum-chemistry and given in `map.xml`. The values are written
 160 to the `state.sql` using the calculator `einternal` (see also internal energy):

Intramolecular reorganization energies

```
| ctp_run -o options.xml -f state.sql -e einternal
```

161 2.5.2 Outersphere reorganization energy

sec:outersphere

162 During the charge transfer reaction, also the molecules outside the charge transfer complex reori-
 163 ent and polarize in order to adjust for changes in electric potential, resulting in the outersphere
 164 contribution to the reorganization energy. $\lambda_{ij}^{\text{out}}$ is particularly important if charge transfer occurs
 165 in a polarizable environment. Assuming that charge transfer is much slower than electronic pol-
 166 arization but much faster than nuclear rearrangement of the environment, $\lambda_{ij}^{\text{out}}$ can be calculated
 167 from the electric displacement fields created by the charge transfer complex [14]

$$\lambda_{ij}^{\text{out}} = \frac{c_p}{2\epsilon_0} \int_{V^{\text{out}}} dV \left[\vec{D}_I(\vec{r}) - \vec{D}_F(\vec{r}) \right]^2, \quad (2.2)$$

equ:lambda_outer1

168 where ϵ_0 is the the permittivity of free space, $\vec{D}_{I,F}(\vec{r})$ are the electric displacement fields created
 169 by the charge transfer complex in the initial (charge on molecule i) and final (charge transferred
 170 to molecule j) states, V^{out} is the volume outside the complex, and $c_p = \frac{1}{\epsilon_{\text{opt}}} - \frac{1}{\epsilon_s}$ is the Pekar factor,
 171 which is determined by the low (ϵ_s) and high (ϵ_{opt}) frequency dielectric permittivities.

172 Eq. (2.2) can be simplified by assuming spherically symmetric charge distributions on molecules
 173 i and j with total charge e . Integration over the volume V^{out} outside of the two spheres of radii R_i
 174 and R_j centered on molecules i and j leads to the classical Marcus expression for the outersphere
 175 reorganization energy

$$\lambda_{ij}^{\text{out}} = \frac{c_p e^2}{4\pi\epsilon_0} \left(\frac{1}{2R_i} + \frac{1}{2R_j} - \frac{1}{r_{ij}} \right), \quad (2.3)$$

equ:lambda_outer2

176 where r_{ij} is the molecular separation. While eq. (2.3) captures the main physics, e.g. predicts
 177 smaller outer-sphere reorganization energies (higher rates) for molecules at smaller separations,

178 it often cannot provide quantitative estimates, since charge distributions are rarely spherically
179 symmetric.

180 Alternatively, the displacement fields can be constructed using the atomic partial charges. The
181 difference of the displacement fields at the position of an atom b_k outside the charge transfer
182 complex (molecule $k \neq i, j$) can be expressed as

$$\vec{D}_I(\vec{r}_{b_k}) - \vec{D}_F(\vec{r}_{b_k}) = \sum_{a_i} \frac{q_{a_i}^c - q_{a_i}^n}{4\pi} \frac{(\vec{r}_{b_k} - \vec{r}_{a_i})}{|\vec{r}_{b_k} - \vec{r}_{a_i}|^3} + \sum_{a_j} \frac{q_{a_j}^n - q_{a_j}^c}{4\pi} \frac{(\vec{r}_{b_k} - \vec{r}_{a_j})}{|\vec{r}_{b_k} - \vec{r}_{a_j}|^3}, \quad (2.4)$$

183 where $q_{a_i}^n$ ($q_{a_i}^c$) is the partial charge of atom a of the neutral (charged) molecule i in vacuum. The
184 partial charges of neutral and charged molecules are obtained by fitting their values to reproduce
185 the electrostatic potential of a single molecule (charged or neutral) in vacuum. Assuming a uni-
186 form density of atoms, the integration in eq. (2.2) can be rewritten as a density-weighted sum
187 over all atoms excluding those of the charge transfer complex.

188 The remaining unknown needed to calculate $\lambda_{ij}^{\text{out}}$ is the Pekar factor, c_p . In polar solvents $\epsilon_s \gg$
189 $\epsilon_{\text{opt}} \sim 1$ and c_p is of the order of 1. In most organic semiconductors, however, molecular orien-
190 tations are fixed and therefore the low frequency dielectric permittivity is of the same order of
191 magnitude as ϵ_{opt} . Hence, c_p is small and its value is very sensitive to differences in the permit-
192 tivities.

193 Outersphere reorganization energies for all pairs of molecules in the **neighbor list** can be com-
194 puted from the atomistic trajectory by using the **eoutersphere calculator**.

195 Two methods can be used to compute $\lambda_{ij}^{\text{out}}$. The first method uses the atomistic partial charges of
196 neutral and charged molecules from files specified in `map.xml` and eq. (2.2). The Pekar factor c_p
197 and a cutoff radius based on molecular centers of mass have to be specified in the `options.xml`
198 file.

199 If this method is computationally prohibitive, $\lambda_{ij}^{\text{out}}$ can be computed using eq. (2.3), which as-
200 sumes spherical charge distributions on the molecules. In this case the radii of these spheres are
201 specified in `segments.xml`, while the Pekar factor c_p is given in the `options.xml` file and no
202 cutoff radius is needed.

203 The outer sphere reorganization energies are saved to the `state.sql` file:



Outersphere reorganization energy

```
| ctp_run -o options.xml -f state.sql -e outersphere
```

204 2.6 Site energies

sec:site_energies

205 A charge transfer reaction between molecules i and j is driven by the site energy difference,
206 $\Delta E_{ij} = E_i - E_j$. Since the transfer rate, ω_{ij} , depends exponentially on ΔE_{ij} (see eq. (2.31)) it is
207 important to compute its distribution as accurately as possible. The total site energy difference
208 has contributions due to **externally applied electric field**, electrostatic interactions, polarization
209 effects, and **internal energy** differences. In what follows we discuss how to estimate these contri-
210 butions by making use of first-principles calculations and polarizable force-fields.

211 2.6.1 Externally applied electric field

sec:ext_field

212 The contribution to the total site energy difference due to an external electric field \vec{F} is given by
213 $\Delta E_{ij}^{\text{ext}} = q\vec{F} \cdot \vec{r}_{ij}$, where $q = \pm e$ is the charge and $\vec{r}_{ij} = \vec{r}_i - \vec{r}_j$ is a vector connecting molecules
214 i and j . For typical distances between small molecules, which are of the order of 1 nm, and
215 moderate fields of $F < 10^8$ V/m this term is always smaller than 0.1 eV.

2.6.2 Internal energy

The contribution to the site energy difference due to different internal energies (see figure 2.3) can be written as

$$\Delta E_{ij}^{\text{int}} = \Delta U_i - \Delta U_j = (U_i^{cC} - U_i^{nN}) - (U_j^{cC} - U_j^{nN}), \quad (2.5)$$

where $U_i^{cC(nN)}$ is the total energy of molecule i in the charged (neutral) state and geometry. ΔU_i corresponds to the adiabatic ionization potential (or electron affinity) of molecule i , as shown in figure 2.3. For one-component systems and negligible conformational changes $\Delta E_{ij}^{\text{int}} = 0$, while it is significant for donor-acceptor systems.

Internal energies determined using quantum-chemistry need to be specified in `map.xml`. The values are written to the `state.sql` using the calculator `einternal` (see also `intramolecular reorganization energy`):



Internal energies

```
! ctp_run -o options.xml -f state.sql -e einternal
```

2.6.3 Electrostatic interaction energy

We represent the molecular charge density by choosing multiple expansion sites (“polar sites”) per molecule in such a way as to accurately reproduce the molecular electrostatic potential (ESP), with a set of suitably chosen multipole moments $\{Q_{lk}^a\}$ (in spherical-tensor notation) allocated to each site. The expression for the electrostatic interaction energy between two molecules A and B in the multi-point expansion includes an implicit sum over expansion sites $a \in A$ and $b \in B$,

$$U_{AB} = \sum_{a \in A} \sum_{b \in B} \hat{Q}_{l_1 k_1}^a T_{l_1 k_1 l_2 k_2}^{a,b} \hat{Q}_{l_2 k_2}^b \equiv \hat{Q}_{l_1 k_1}^a T_{l_1 k_1 l_2 k_2}^{a,b} \hat{Q}_{l_2 k_2}^b, \quad (2.6)$$

where we have used the Einstein sum convention for the site indices a and b on the right-hand side of the equation, in addition to the sum convention that is in place for the multipole-moment components $t \equiv l_1 k_1$ and $u \equiv l_2 k_2$. The $T_{l_1 k_1 l_2 k_2}^{a,b}$ are tensors that mediate the interaction between a multipole component $l_1 k_1$ on site a with the moment $l_2 k_2$ on site b . If we include the molecular environment into a perturbative term W to enter in the single-molecule Hamiltonian, the above expression is exactly the first-order correction to the energy where the quantum-mechanical detail has been absorbed in classical multipole moments.

There are a number of strategies how to arrive at such a collection of *distributed multipoles*. They can be classified according to whether the multipoles are derived (a) from the electrostatic potential generated by the SCF charge density or (b) from a decomposition of the wavefunction itself. Here, we will only draft two of those approaches, CHELPG [15] from category (a) and DMA [16] from category (b).

The CHELPG (CHarges from ELEctrostatic Potentials, Grid-based) method relies on performing a least-squares fit of atom-placed charges to reproduce the electrostatic potential as evaluated from the SCF density on a regularly spaced grid [15]. The fitted charges result from minimizing the Lagrangian function [17]

$$z(\{q_i\}) = \sum_{k=1}^M \left(\phi(\vec{r}_k) - \sum_{i=1}^N \frac{1}{4\pi\epsilon_0} \frac{q_i}{|\vec{r}_i - \vec{r}_k|} \right) + \lambda \left(q_{\text{mol}} - \sum_{i=1}^N q_i \right), \quad (2.7)$$

with M grid points, N atomic sites, the set of atomic partial charges $\{q_i\}$ and the SCF potential ϕ . The Lagrange multiplier λ constrains the sum of the fitted charges to the molecular charge q_{mol} . The main difference from other fitting schemes [18] is the algorithm that selects the positions

at which the potential is evaluated (we note that the choice of grid points can have substantial effects especially for bulky molecules). Clearly, the CHELPG method can be (and has been) extended to include higher atomic multipoles. It should be noted, however, how already the inclusion of atomic dipoles hardly improves the parametrization, and can in fact be harmful to its conformational stability.

The Distributed-Multipole-Analysis (DMA) approach [16, 19], developed by A. Stone, operates directly on the quantum-mechanical density matrix, expanded in terms of atom- and bond-centered Gaussian functions $\chi_\alpha = R_{LK}(\vec{x} - \vec{s}_\alpha) \exp[-\zeta(\vec{x} - \vec{s}_\alpha)^2]$,

$$\rho(\vec{x}) = \sum_{\alpha,\beta} \rho_{\alpha\beta} \chi_\alpha(\vec{x} - \vec{s}_\alpha) \chi_\beta(\vec{x} - \vec{s}_\beta). \quad (2.8)$$

The aim is to compute multipole moments according in a distributed fashion: If we use that the overlap product $\chi_\alpha \chi_\beta$ of two Gaussian basis functions yields itself a Gaussian centered at $\vec{P} = (\zeta_\alpha \vec{s}_\alpha + \zeta_\beta \vec{s}_\beta) / (\zeta_\alpha + \zeta_\beta)$, it is possible to proceed in two steps: First, we compute the multipole moments associated with a specific summand in the density matrix, referred to the overlap center \vec{P} :

$$Q_{LK}[\vec{P}] = - \int R_{LK}(\vec{x} - \vec{P}) \rho_{\alpha\beta} \chi_\alpha \chi_\beta d^3x. \quad (2.9)$$

Second, we transfer the resulting $Q_{lk}[\vec{P}]$ to the position \vec{S} of a polar site according to the rule [16]

$$Q_{nm}[\vec{S}] = \sum_{l=0}^L \sum_{k=-l}^l \left[\binom{n+m}{l+k} \binom{n-m}{l-k} \right]^{1/2} R_{n-l,m-k}(\vec{S} - \vec{P}) \cdot Q_{lk}[\vec{P}]. \quad (2.10)$$

Note how this requires a rule for the choice of the expansion site to which the multipole moment should be transferred. In the near past [19], the nearest-site algorithm, which allocates the multipole moments to the site closest to the overlap center, was replaced for diffuse functions by an algorithm based on a smooth weighting function in conjunction with grid-based integration methods in order to decrease the basis-set dependence of the resulting set of distributed multipoles.

One important advantage of the DMA approach over fitting algorithms such as CHELPG or Merz-Kollman (MK) is that higher-order moments can also be derived without too large an ambiguity.

The ‘mps’ file format used by VOTCA for the definition of distributed multipoles (as well as point polarizabilities, see subsequent section) is based on the GDMA punch format of A. Stone’s GDMA program [19] (the punch output file can be immediately plugged into VOTCA without any conversions to be applied). Furthermore the log-file of different QM packages (currently Gaussian, Turbomole and NWChem) may be fed into the `log2mps tool`, which will subsequently generate the appropriate mps-file.



Read in ESP charges from a QM log file

```
| ctp_tools -o options.xml -e log2mps
```

2.6.4 Induction energy - the Thole model

If we in addition to the permanent set of multipole moments $\{Q_t^a\}$ allow for induced moments $\{\Delta Q_t^a\}$ and penalize their generation with a bilinear form (giving rise to a strictly positive contribution to the energy),

$$U_{\text{int}} = \frac{1}{2} \sum_A \Delta Q_t^a \eta_{tt'}^{aa'} \Delta Q_{t'}^{a'}, \quad (2.11)$$

it can be shown that the induction contribution to the site energy evaluates to an expression where all interactions between induced moments have cancelled out, and interactions between permanent and induced moments are scaled down by 1/2 [20]:

$$U_{pu} = \frac{1}{2} \sum_A \sum_{B>A} [\Delta Q_t^a T_{tu}^{ab} Q_u^b + \Delta Q_t^b T_{tu}^{ab} Q_u^a]. \quad (2.12) \quad \text{equ:u_pu}$$

This term can be viewed as the second-order (induction) correction to the molecular interaction energy. The sets of $\{Q_t^a\}$ are solved for self-consistently via

$$\Delta Q_t^a = - \sum_{B \neq A} \alpha_{tt'}^{aa'} T_{t'u}^{a'b} (Q_u^b + \Delta Q_u^b), \quad (2.13) \quad \text{equ:self_consistent_dQ}$$

263 where the polarizability tensors $\alpha_{tt'}^{aa'}$ are given by the inverse of $\eta_{tt'}^{aa'}$.
 264 With eqs. 2.13 and 2.12 we have at hand expressions that allow us to compute the induction en-
 265 ergy contribution to site energies in an iterative manner based on a set of molecular distributed
 266 multipoles $\{Q_t^a\}$ and polarizabilities $\{\alpha_{tt'}^{aa'}\}$. We have drafted in the previous section how to ob-
 267 tain the former from a wavefunction decomposition or fitting scheme (GDMA, CHELPG). The
 268 $\{\alpha_{tt'}^{aa'}\}$ can be derived formally (or rather: read off) from a perturbative expansion of the molec-
 269 ular interaction. In this work we make use of the Thole model [21, 22] as a semi-empirical ap-
 270 proach to obtain the sought-after point polarizabilities in the local dipole approximation, that is,
 271 $[\alpha_{tt'}^{aa'}] = \alpha_{tt'}^{aa'} \delta_{t\beta} \delta_{t'\beta} \delta_{aa'}$, where $\beta \in \{x, y, z\}$ references the dipole-moment component.
 272 The Thole model is based on a modified dipole-dipole interaction, which can be reformulated in
 273 terms of the interaction of smeared charge densities. This has been shown to be necessary due
 274 to the divergent head-to-tail dipole-dipole interaction that otherwise results at small intersepara-
 275 tions on the Å scale [21–23]. Smearing out the charge distribution mimics the nature of the QM
 276 wavefunction, which effectively guards against this unphysical polarization catastrophe. Since
 277 the point dipoles however only react individually to the external field, any correlation effects as
 278 were still accounted for in the $\{\alpha_{tt'}^{aa'}\}$ are lost, except perhaps those correlations that are due to
 279 the mere classical field interaction.

The smearing of the nuclei-centered multipole moments is obtained via a fractional charge den-
 sity $\rho_f(\vec{u})$ which should be normalized to unity and fall off rapidly as of a certain radius $\vec{u} = \vec{u}(\vec{R})$.
 The latter is related to the physical distance vector \vec{R} connecting two interacting sites via a linear
 scaling factor that takes into account the magnitude of the isotropic site polarizabilities α^a . This
 isotropic fractional charge density gives rise to a modified potential

$$\phi(u) = - \frac{1}{4\pi\epsilon_0} \int_0^u 4\pi u' \rho(u') du' \quad (2.14) \quad \text{equ:mod_potential}$$

We can relate the multipole interaction tensor $T_{ij\dots}$ (this time in Cartesian coordinates) to the
 fractional charge density in two steps: First, we rewrite the tensor in terms of the scaled distance
 vector \vec{u} ,

$$T_{ij\dots}(\vec{R}) = f(\alpha^a \alpha^b) t_{ij\dots}(\vec{u}(\vec{R}), \alpha^a \alpha^b), \quad (2.15)$$

where the specific form of $f(\alpha^a \alpha^b)$ results from the choice of $u(\vec{R}, \alpha^a \alpha^b)$. Second, we demand
 that the smeared interaction tensor $t_{ij\dots}$ is given as usual by the appropriate derivative of the
 potential in eq. 2.14,

$$t_{ij\dots}(\vec{u}) = -\partial_{u_i} \partial_{u_j} \dots \phi(\vec{u}). \quad (2.16)$$

280 It turns out that for a suitable choice of $\rho_f(\vec{u})$, the modified interaction tensors can be rewritten
 281 in such a way that powers n of the distance $R = |\vec{R}|$ are damped with a damping function
 282 $\lambda_n(\vec{u}(\vec{R}))$ [24].

283 There is a large number of fractional charge densities $\rho_f(\vec{u})$ that have been tested for the purpose
 284 of giving best results for the molecular polarizability as well as interaction energies. Note how a
 285 great advantage of the Thole model is the exceptional transferability of the atomic polarizabilities
 286 to compounds not used for the fitting procedure [22]. In fact, for most organic molecules, a fixed
 287 set of atomic polarizabilities ($\alpha_C = 1.334$, $\alpha_H = 0.496$, $\alpha_N = 1.073$, $\alpha_O = 0.873$, $\alpha_S = 2.926 \text{ \AA}^3$)
 288 based on atomic elements yields satisfactory results.

VOTCA implements the Thole model with an exponentially-decaying fractional charge density

$$\rho(u) = \frac{3a}{4\pi} \exp(-au^3), \quad (2.17)$$

289 where $\vec{u}(\vec{R}, \alpha^a \alpha^b) = \vec{R}/(\alpha^a \alpha^b)^{1/6}$ and the smearing exponent $a = 0.39$ (which can however be
 290 changed from the program options), as used in the AMOEBA force field [24].

291 Even though the Thole model performs very well for many organic compounds with only the
 292 above small set of element-based polarizabilities, conjugated molecules may require a more in-
 293 tricate parametrization. The simplest approach is to resort to scaled polarizabilities to match
 294 the effective molecular polarizable volume $V \sim \alpha_x \alpha_y \alpha_z$ as predicted by QM calculations (here
 295 $\alpha_x, \alpha_y, \alpha_z$ are the eigenvalues of the molecular polarizability tensor). The `molpol` tool assists
 296 with this task, it self-consistently calculates the Thole polarizability for an input `mps`-file and
 297 optimizes (if desired) the atomic polarizabilities in the above simple manner.

Generate Thole-type polarizabilities for a segment

```
| ctp_tools -o options.xml -e molpol
```

298 The electrostatic and induction contribution to the site energy is evaluated by the `emultipole`
 299 `calculator`. Atomistic partial charges for charged and neutral molecules are taken from `mps`-files
 300 (extended GDMA format) specified in `map.xml`. Note that, in order to speed up calculations for
 301 both methods, a cut-off radius (for the molecular centers of mass) can be given in `options.xml`.
 302 Threaded execution is advised.

Electrostatic and induction corrections

```
| ctp_run -o options.xml -f state.sql -e emultipole
```

303 Furthermore available are `zmultipole`, which extends `emultipole` to allow for an electrostatic
 304 buffer layer (loosely related to the z-buffer in OpenGL, hence the name) and anisotropic point
 305 polarizabilities. For the interaction energy of charged clusters of any user-defined composition
 306 (Frenkel states, CT states, ...), `xqmultipole` can be used.

Interaction energy of charged molecular clusters embedded in a molecular environment

```
| ctp_parallel -o options.xml -f state.sql -e xqmultipole
```

307 2.6.5 Long-range Coulomb interactions

sec:ewald

308 This section is a practical guide for doing electrostatic calculations in slabs using aperiodic Ewald
 309 scheme described in [1].

310 First, you will need to generate the required quantum mechanical reference, comprising molecu-
 311 lar charge density and polarizability for all charge states (neutral, cationic, anionic). For example,
 312 you can use GAUSSIAN to do this:

```
313 ...  

  314 #p b3lyp/6-31+g(d,p) pop(full, chelpg) polar(dipole) nosymm test  

  315 ...  

  316
```

317 Afterwords, you have to generate all required *mps*-files with distributed multipoles and polariz-
 318 abilities. The options file should point to the QM *log*-files, as well as contain the target molecular
 319 polarizability tensor in upper-diagonal order *xx xy xz yy yz zz* in units of \AA^3 .

```
320 $ ctp_tools -e log2mps -o options.xml
321 $ ctp_tools -e molpol -o options.xml
322
323 <options>
324   <log2mps>
325     <package>gaussian</package>
326     <logfile>input.log</logfile>
327     <mpsfile></mpsfile>
328   </log2mps>
329   <molpol>
330     <mpsfiles>
331       <input>input.mps</input>
332       <output>output.mps</output>
333       <polar>output.xml</polar>
334     </mpsfiles>
335     <induction>
336       <expdamp>0.39000</expdamp>
337       <wSOR>0.30000</wSOR>
338       <maxiter>1024</maxiter>
339       <tolerance>0.00001</tolerance>
340     </induction>
341     <target>
342       <optimize>>true</optimize>
343       <molpol>77 0 0 77 0 77</molpol>
344       <tolerance>0.00001</tolerance>
345     </target>
346   </molpol>
347 </options>
348
```

349 Next, generate the *mps* table, which relates the state of the molecule (neutral, cation, anion) with
 350 a corresponding electrostatic representation. This is provided by the *stateserver*. The resulting
 351 output file has the default name “mps.tab”:

```
352 $ ctp_run -e stateserver -o options.xml -f state.sql
353
354 <options>
355   <stateserver>
356     <keys>mps</keys>
357   </stateserver>
358 </options>
```

359 Next, generate the job file. This job file lists the electrostatic configurations that are to be investi-
 360 gated. It can either be composed by hand or generated automatically from the *sql* file via the *job-*
 361 *writer*, which at present takes either “mps.chrg”, “mps.single” or “mps.ct” as key, where the latter
 362 resorts to a neighbor list. The resulting *xml*-file has the default name “jobwriter.mps.chrg.xml”.

```
363 $ ctp_run -e jobwriter -o options.xml -f state.sql
364
365 <options>
366   <jobwriter>
367     <keys>mps.chrg</keys>
```

```

368 <single_id>10</single_id>
369 <cutoff>3</cutoff>
370 </jobwriter>
371 </options>

```

372 The input string in the job file for the long-range corrected calculators has the same format as for
 373 the *xqmultipole* calculator, “id1:name1:mps1 id2:name2:mps2 ...”. See sample below.

```

374 <jobs>
375   <job>
376     <id>1</id>
377     <tag>1e:2h</tag>
378     <input>1:spl:MP_FILES/spl_e.mps 2:spl:MP_FILES/spl_h.mps</input>
379     <status>AVAILABLE</status>
380   </job>
381   <job>
382     ...
383   </job>
384     ...
385 </jobs>

```

386 Next, generate the *ptop*-file that stores the induction state of the neutral *background*. The responsi-
 387 ble *ewdbgp01* calculator can be run in a threaded fashion, depending on system size. The resulting
 388 *ptop*-file has the default name “bgp_main.ptop”.

```

389 $ ctp_run -e ewdbgp01 -o options.xml -f state.sql -t 8

```

```

390
391 <options>
392   <ewdbgp01>
393     <multipoles>system.xml</multipoles>
394     <control>
395       <mps_table>mps.tab</mps_table>
396       <pdb_check>1</pdb_check>
397     </control>
398     <coulombmethod>
399       <method>ewald</method>
400       <cutoff>6</cutoff>
401       <shape>xyslab</shape>
402     </coulombmethod>
403     <polarmethod>
404       <method>thole</method>
405       <wSOR_N>0.350</wSOR_N>
406       <aDamp>0.390</aDamp>
407     </polarmethod>
408     <convergence>
409       <energy>1e-05</energy>
410       <kfactor>100</kfactor>
411       <rfactor>6</rfactor>
412     </convergence>
413   </ewdbgp01>
414 </options>

```

415 Finally, run the energy computation using *pewald3d*. This job calculator is wrapped by the *ctp_parallel*
 416 executable, which allows for communication between different processes via the job and state file.
 417 Unfortunately, communication, though guarded by a file lock, may fail on some architectures in
 418 the event of frequent accesses to the job file. This frequency can be controlled by the *-c/-cache*

419 argument, which defines the number of jobs that are loaded in *one* batch by a specific process/n-
420 ode.

```
421 $ ctp_parallel -e pewald3d -o options.xml -f /absolute/path/to/state.sql -s 0 -t 8 -c
```

```
422
423 <options>
424   <ewald>
425     <jobcontrol>
426       <job_file>/absolute/path/to/jobs.xml</job_file>
427     </jobcontrol>
428     <multipoles>
429       <mapping>system.xml</mapping>
430       <mps_table>mps.tab</mps_table>
431       <polar_bg>bgp_main.ptop</polar_bg>
432       <pdb_check>0</pdb_check>
433     </multipoles>
434     <coulombmethod>
435       <method>ewald</method>
436       <cutoff>8</cutoff>
437       <shape>xyslab</shape>
438       <save_nblast>>false</save_nblast>
439     </coulombmethod>
440     <polarmethod>
441       <method>thole</method>
442       <induce>1</induce>
443       <cutoff>4</cutoff>
444       <tolerance>0.001</tolerance>
445       <radial_dielectric>4.0</radial_dielectric>
446     </polarmethod>
447     <tasks>
448       <calculate_fields>>true</calculate_fields>
449       <polarize_fg>>true</polarize_fg>
450       <evaluate_energy>>true</evaluate_energy>
451       <apply_radial>>false</apply_radial>
452     </tasks>
453     <coarsegrain>
454       <cg_background>>false</cg_background>
455       <cg_foreground>>false</cg_foreground>
456       <cg_radius>3</cg_radius>
457       <cg_anisotropic>>true</cg_anisotropic>
458     </coarsegrain>
459     <convergence>
460       <energy>1e-05</energy>
461       <kfactor>100</kfactor>
462       <rfactor>6</rfactor>
463     </convergence>
464   </ewald>
465 </options>
```

466 Parse the output. The results from the computation are stored in the same job file that was sup-
467 plied to the calculator. The key data is provided in the *output/summary* section and consists of the
468 electrostatic and induction contributions *output/summary/eindu* and *output/summary/estat*. Note
469 that only configuration energy *differences* carry meaning. The parsing is best done by script, as
470 the “-j/-jobs read” option for *pewald3d* is not yet implemented.

```

471 <jobs>
472   <job>
473     <id>1</id>
474     <tag>1e:2h</tag>
475     <input>1:spl:MP_FILES/spl_e.mps 2:spl:MP_FILES/spl_h.mps</input>
476     <status>COMPLETE</status>
477     <host>thop76:5476</host>
478     <time>17:22:56</time>
479     <output>
480       <summary>
481         <type>neutral</type>
482         <xyz unit="nm">-0.1750000 -0.1750000 -5.4250000</xyz>
483         <total unit="eV">-3.2112834</total>
484         <estat unit="eV">-2.3753255</estat>
485         <eindu unit="eV">-0.8359579</eindu>
486       </summary>
487       <terms_i>
488         <F-00-01-11>-3.32999e+00 -3.32481e-01 +4.06829e-02</F-00-01-11>
489         <M-00-11--->+1.33689e-01 +4.74490e-01</M-00-11--->
490         <E-PP-PU-UU>-2.37533e+00 -7.37812e-01 -2.73212e-18</E-PP-PU-UU>
491       </terms_i>
492       <terms_o>
493         <R-pp-pu-uu>-1.89357e-01 = +2.69583e-08 ...</R-pp-pu-uu>
494         <K-pp-pu-uu>-7.31703e-03 = -2.69583e-08 ...</K-pp-pu-uu>
495         <O-pp-pu-uu>+0.00000e+00 = +0.00000e+00 ...</O-pp-pu-uu>
496         <J-pp-pu-uu>+5.14048e-04 = -2.99187e-17 ...</J-pp-pu-uu>
497         <C-pp-pu-uu>+1.51186e-03 = +0.00000e+00 ...</C-pp-pu-uu>
498         <Q-pp-pu-uu>+0.00000e+00 = +0.00000e+00 ...</Q-pp-pu-uu>
499       </terms_o>
500       <shells>
501         <FGC>1874</FGC>
502         <FGN>1874</FGN>
503         <MGN>54429</MGN>
504         <BGN>36</BGN>
505         <BGP>52</BGP>
506         <QM0>2</QM0>
507         <MM1>1872</MM1>
508         <MM2>0</MM2>
509       </shells>
510       <timing>
511         <t_total unit="min">5.29</t_total>
512         <t_wload unit="min">0.00 2.24 0.88 2.18</t_wload>
513       </timing>
514     </output>
515   </job>
516   <job>
517     ...
518   </job>
519   ...
520 </jobs>
521

```

2.7 Transfer integrals

The electronic transfer integral element J_{ij} entering the Marcus rates in eq. (2.31) is defined as

$$J_{ij} = \langle \phi_i | \hat{H} | \phi_j \rangle, \quad (2.18) \quad \text{equ:TI}$$

where ϕ_i and ϕ_j are diabatic wavefunctions, localized on molecule i and j respectively, participating in the charge transfer, and \hat{H} is the Hamiltonian of the formed dimer. Within the frozen-core approximation, the usual choice for the diabatic wavefunctions ϕ_i is the highest occupied molecular orbital (HOMO) in case of hole transport, and the lowest unoccupied molecular orbital (LUMO) in the case of electron transfer, while \hat{H} is an effective single particle Hamiltonian, e.g. Fock or Kohn-Sham operator of the dimer. As such, J_{ij} is a measure of the strength of the electronic coupling of the frontier orbitals of monomers mediated by the dimer interactions.

Intrinsically, the transfer integral is very sensitive to the molecular arrangement, i.e. the distance and the mutual orientation of the molecules participating in charge transport. Since this arrangement can also be significantly influenced by static and/or dynamic disorder [25–29], it is essential to calculate J_{ij} explicitly for each hopping pair within a realistic morphology. Considering that the number of dimers for which eq. (2.18) has to be evaluated is proportional to the number of molecules times their coordination number, computationally efficient and at the same time quantitatively reliable schemes are required.

2.7.1 Projection of monomer orbitals on dimer orbitals (DIPRO)

An approach for the determination of the transfer integral that can be used for any single-particle electronic structure method (Hartree-Fock, DFT, or semiempirical methods) is based on the projection of monomer orbitals on a manifold of explicitly calculated dimer orbitals. This dimer projection (DIPRO) technique including an assessment of computational parameters such as the basis set, exchange-correlation functionals, and convergence criteria is presented in detail in ref. [5]. A brief summary of the concept is given below.

We start from an effective Hamiltonian ¹

$$\hat{H}^{\text{eff}} = \sum_i \epsilon_i \hat{a}_i^\dagger \hat{a}_i + \sum_{j \neq i} J_{ij} \hat{a}_i^\dagger \hat{a}_j + c.c. \quad (2.19) \quad \text{equ:dipro_eq1}$$

where \hat{a}_i^\dagger and \hat{a}_i are the creation and annihilation operators for a charge carrier located at the molecular site i . The electron site energy is given by ϵ_i , while J_{ij} is the transfer integral between two sites i and j . We label their frontier orbitals (HOMO for hole transfer, LUMO for electron transfer) ϕ_i and ϕ_j , respectively. Assuming that the frontier orbitals of a dimer (adiabatic energy surfaces) result exclusively from the interaction of the frontier orbitals of monomers, and consequently expand them in terms of ϕ_i and ϕ_j . The expansion coefficients, $\bar{\mathbf{C}}$, can be determined by solving the secular equation

$$(\mathbf{H} - E\mathbf{S})\bar{\mathbf{C}} = 0 \quad (2.20) \quad \text{equ:dipro_eq2}$$

where \mathbf{H} and \mathbf{S} are the Hamiltonian and overlap matrices of the system, respectively. These matrices can be written explicitly as

$$\mathbf{H} = \begin{pmatrix} e_i & H_{ij} \\ H_{ij}^* & e_j \end{pmatrix} \quad \mathbf{S} = \begin{pmatrix} 1 & S_{ij} \\ S_{ij}^* & 1 \end{pmatrix} \quad (2.21) \quad \text{equ:dipro_eq3}$$

with

$$\begin{aligned} e_i &= \langle \phi_i | \hat{H} | \phi_i \rangle & H_{ij} &= \langle \phi_i | \hat{H} | \phi_j \rangle \\ e_j &= \langle \phi_j | \hat{H} | \phi_j \rangle & S_{ij} &= \langle \phi_j | \phi_i \rangle \end{aligned} \quad (2.22) \quad \text{equ:dipro_eq4}$$

¹we use following notations: a - number, $\bar{\mathbf{a}}$ - vector, \mathbf{A} - matrix, \hat{A} - operator

556 The matrix elements $e_{i(j)}$, H_{ij} , and S_{ij} entering eq. (2.21) can be calculated via projections on the
 557 dimer orbitals (eigenfunctions of \hat{H}) $\{|\phi_n^D\rangle\}$ by inserting $\hat{1} = \sum_n |\phi_n^D\rangle\langle\phi_n^D|$ twice. We exemplify
 558 this explicitly for H_{ij} in the following

$$H_{ij} = \sum_{nm} \langle\phi_i|\phi_n^D\rangle\langle\phi_n^D|\hat{H}|\phi_m^D\rangle\langle\phi_m^D|\phi_j\rangle. \quad (2.23) \quad \text{eq:dipro_eq16}$$

559 The Hamiltonian is diagonal in its eigenfunctions, $\langle\phi_n^D|\hat{H}|\phi_m^D\rangle = E_n\delta_{nm}$. Collecting the projec-
 560 tions of the frontier orbitals $|\phi_{i(j)}\rangle$ on the n -th dimer state $(\bar{\mathbf{V}}_{(i)})_n = \langle\phi_i|\phi_n^D\rangle$ and $(\bar{\mathbf{V}}_{(j)})_n =$
 561 $\langle\phi_j|\phi_n^D\rangle$ respectively, into vectors we obtain

$$H_{ij} = \bar{\mathbf{V}}_{(i)} \mathbf{E} \bar{\mathbf{V}}_{(j)}^\dagger. \quad (2.24) \quad \text{eq:dipro_eq17}$$

562 What is left to do is determine these projections $\bar{\mathbf{V}}_{(k)}$. In all practical calculations the molecular
 563 orbitals are expanded in basis sets of either plane waves or of localized atomic orbitals $|\varphi_\alpha\rangle$.
 564 We will first consider the case that the calculations for the monomers are performed using a
 565 counterpoise basis set that is commonly used to deal with the basis set superposition error (BSSE).
 566 The basis set of atom-centered orbitals of a monomer is extended to the one of the dimer by
 567 adding the respective atomic orbitals at virtual coordinates of the second monomer. We can then
 568 write the respective expansions as

$$|\phi_k\rangle = \sum_\alpha \lambda_\alpha^{(k)} |\varphi_\alpha\rangle \quad \text{and} \quad |\phi_n^D\rangle = \sum_\alpha D_\alpha^{(n)} |\varphi_\alpha\rangle \quad (2.25) \quad \text{eq:dipro_eq18}$$

569 where $k = i, j$. The projections can then be determined within this common basis set as

$$(\bar{\mathbf{V}}_k)_n = \langle\phi_k|\phi_n^D\rangle = \sum_\alpha \lambda_\alpha^{(k)} \langle\alpha|\sum_\beta D_\beta^{(n)}|\beta\rangle = \bar{\lambda}_{(k)}^\dagger \mathcal{S} \bar{\mathbf{D}}_{(n)} \quad (2.26) \quad \text{eq:dipro_eq19}$$

570 where \mathcal{S} is the overlap matrix of the atomic basis functions. This allows us to finally write the
 571 elements of the Hamiltonian and overlap matrices in eq. (2.21) as:

$$\begin{aligned} H_{ij} &= \bar{\lambda}_{(i)}^\dagger \mathcal{S} \mathbf{E} \mathbf{D} \mathbf{E}^\dagger \mathcal{S}^\dagger \bar{\lambda}_{(j)} \\ S_{ij} &= \bar{\lambda}_{(i)}^\dagger \mathcal{S} \mathbf{D} \mathbf{D}^\dagger \mathcal{S}^\dagger \bar{\lambda}_{(j)} \end{aligned} \quad (2.27) \quad \text{eq:dipro_eq20}$$

572 Since the two monomer frontier orbitals that form the basis of this expansion are not orthogonal
 573 in general ($\mathbf{S} \neq \mathbf{1}$), it is necessary to transform eq. (2.20) into a standard eigenvalue problem of
 574 the form

$$\mathbf{H}^{\text{eff}} \bar{\mathbf{C}}^{\text{eff}} = \mathbf{E} \bar{\mathbf{C}}^{\text{eff}} \quad (2.28) \quad \text{eq:dipro_eq7}$$

575 to make it correspond to eq. (2.19). According to Löwdin such a transformation can be achieved
 576 by

$$\mathbf{H}^{\text{eff}} = \mathbf{S}^{-1/2} \mathbf{H} \mathbf{S}^{-1/2}. \quad (2.29) \quad \text{eq:dipro_eq9}$$

577 This then yields an effective Hamiltonian matrix in an orthogonal basis, and its entries can di-
 578 rectly be identified with the site energies ϵ_i and transfer integrals J_{ij} :

$$\mathbf{H}^{\text{eff}} = \begin{pmatrix} e_i^{\text{eff}} & H_{ij}^{\text{eff}} \\ H_{ij}^{*\text{eff}} & e_j^{\text{eff}} \end{pmatrix} = \begin{pmatrix} \epsilon_i & J_{ij} \\ J_{ij}^* & \epsilon_j \end{pmatrix} \quad (2.30) \quad \text{eq:dipro_eq11}$$

579 2.7.2 DFT-based transfer integrals using DIPRO

sec:dft

580 The calculation of one electronic coupling element based on DFT using the DIPRO method re-
 581 quires the overlap matrix of atomic orbitals \mathcal{S} , the expansion coefficients for monomer $\bar{\lambda}_{(k)} =$
 582 $\{\lambda_\alpha^{(k)}\}$ and dimer orbitals $\bar{\mathbf{D}}_{(n)} = \{D_\alpha^{(n)}\}$, as well as the orbital energies E_n of the dimer are

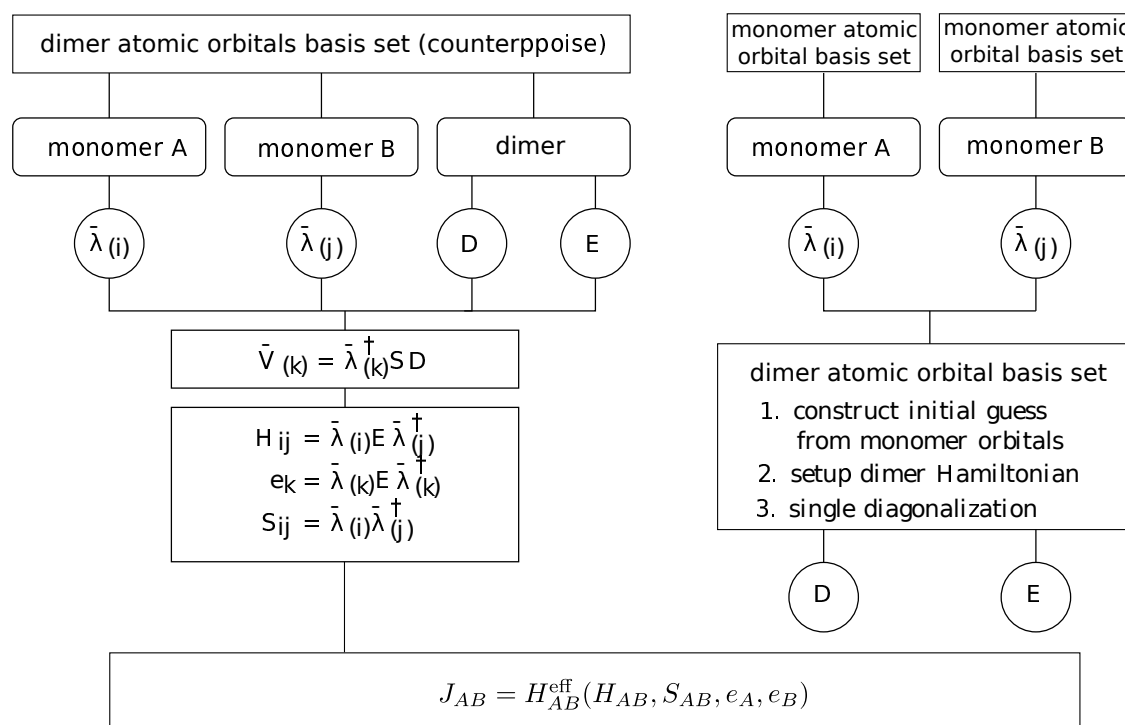


Figure 2.4: Schematics of the DIPRO method. (a) General workflow of the projection technique. (b) Strategy of the efficient noCP+noSCF implementation, in which the monomer calculations are performed independently from the dimer configurations (noCP), using the `edft calculator`. The dimer Hamiltonian is subsequently constructed based on an initial guess formed from monomer orbitals and only diagonalized once (noSCF) before the transfer integral is calculated by projection. This second step is performed by the `idft calculator`.

fig:dipro_scheme

583 required as input. In practical situations, performing self-consistent quantum-chemical calculations
 584 for each individual monomer and one for the dimer to obtain this input data is extremely
 585 demanding. Several simplifications can be made to reduce the computational effort, such as
 586 using non-Counterpoise basis sets for the monomers (thereby decoupling the monomer calculations
 587 from the dimer run) and performing only a single SCF step in a dimer calculation starting
 588 from an initial guess formed from a superposition of monomer orbitals. This "noCP+noSCF"
 589 variant of DIPRO is shown in figure 2.4(a) and recommended for production runs. A detailed
 590 comparative study of the different variants can be found in [5].


591 The code currently contains supports evaluation of transfer integrals from quantum-chemical
 592 calculations performed with the `Gaussian`, `Turbomole`, and `NWChem` packages. The interfacing
 593 procedure consists of three main steps: generation of input files for monomers and dimers,
 594 performing the actual quantum-chemical calculations, and calculating the transfer integrals.

595 Monomer calculations

sec:edft


596 First, `hopping sites` and a `neighbor list` need to be generated from the atomistic topology and
 597 trajectory and written to the `state.sql` file. Then the parallel `edft calculator` manages the
 598 calculation of the monomer properties required for the determination of electronic coupling elements.
 599 Specifically, the individual steps it performs are:

- 600 1. Creation of a job file containing the list of molecules to be calculated with DFT

 **Writing job file for edft**

```
| ctp_parallel -o options.xml -f state.sql -e edft -j write
```

601 2. Running of all jobs in job file

 **Running all edft jobs**

```
| ctp_parallel -o options.xml -f state.sql -e edft -j run
```

602 which includes

- 603 • creating the input files for the DFT calculation (using the package specified in `options.xml`)
- 604 in the directory

605 `OR_FILES/package/frame_F/mol_M`

606 where F is the index of the frame in the trajectory, M is the index of a molecule in this

607 frame,

- 608 • executing the DFT run, and
- 609 • after completion of this run, parsing the output (number of electrons, basis set, molec-
- 610 ular orbital expansion coefficients), and saving it in compressed form to

611 `OR_FILES/molecules/frame_F/molecule_M.orb`

612 **Calculating the transfer integrals**

sec:edft


613 After the monomer calculations have been completed successfully, the respective runs for dimers

614 from the neighborlist can be performed using the parallel `idft calculator`, which manages the

615 DFT runs for the hopping pairs and determines the coupling element using DIPRO. Again, sev-


616 eral steps are required:

617 1. Creation of a job file containing the list of pairs to be calculated with DFT

 **Writing job file for idft**

```
| ctp_parallel -o options.xml -f state.sql -e idft -j write
```

618 2. Running of all jobs in job file

 **Running all idft jobs**

```
| ctp_parallel -o options.xml -f state.sql -e idft -j run
```

619 which includes

- 620 • creating the input files (including the merged guess for a noSCF calculation, if re-
- 621 quested) for the DFT calculation (using the package specified in `options.xml`) in the
- 622 directory

623 `OR_FILES/package/frame_F/pair_M_N`

624 where M and N are the indices of the molecules in this pair,

- 625 • executing the DFT run, and

- after completion of this run, parsing the output (number of electrons, basis set, molecular orbital expansion coefficients and energies, atomic orbital overlap matrix), and saving the pair information in compressed form to

```
OR_FILES/pairs/frame_F/pair_M_N.orb
```

- loading the monomer orbitals from the previously saved *.orb files.
- calculating the coupling elements and write them to the job file

3. Reading the coupling elements from the job file and saving them to the `state.sql` file

633

Saving `idft` results from job file to `state.sql`

```
| ctp_parallel -o options.xml -f state.sql -e idft -j read
```

634 2.7.3 ZINDO-based transfer integrals using MOO

sec:izindo

635 An approximate method based on Zerner's Intermediate Neglect of Differential Overlap (ZINDO)
636 has been described in Ref. [7]. This semiempirical method is substantially faster than first-
637 principles approaches, since it avoids the self-consistent calculations on each individual monomer
638 and dimer. This allows to construct the matrix elements of the ZINDO Hamiltonian of the dimer
639 from the weighted overlap of molecular orbitals of the two monomers. Together with the in-
640 troduction of rigid segments, only a single self-consistent calculation on one isolated conjugated
641 segment is required. All relevant molecular overlaps can then be constructed from the obtained
642 molecular orbitals.

643 The main advantage of the molecular orbital overlap (MOO) library is *fast* evaluation of electronic
644 coupling elements. Note that MOO is based on the ZINDO Hamiltonian which has limited appli-
645 cability. The general advice is to first compare the accuracy of the MOO method to the DFT-based
646 calculations.

647 MOO can be used both in a `standalone mode` and as an `izindo calculator` of VOTCA-CTP.

648 Since MOO constructs the Fock operator of a dimer from the molecular orbitals of monomers by
649 translating and rotating the orbitals of `rigid fragments`, the optimized geometry of all `conjugated`
650 `segments` and the coefficients of the molecular orbitals are required as its input in addition to
651 the state file (`state.sql`) with the `neighbor list`. Coordinates are stored in `geometry.xyz`
652 files with four columns, first being the atom type and the next three atom coordinates. This is a
653 standard `xyz` format without a header. Note that the atom order in the `geometry.xyz` files can
654 be different from that of the mapping files. The correspondence between the two is established
655 in the `map.xml` file.

Attention

Izindo requires the specification of orbitals for hole and electron transport in `map.xml`. They are the HOMO and LUMO respectively and can be retrieved from the `log` file from which the `zindo.orb` file is generated. The number of alpha electrons is the HOMO, the LUMO is HOMO+1

656 The calculated transfer integrals are immediately saved to the `state.sql` file.

Transfer integrals from `izindo`

```
| ctp_run -o options.xml -f state.sql -e izindo
```

2.8 Charge transfer rate

Charge transfer rates can be postulated based on intuitive physical considerations, as it is done in the Gaussian disorder models [25, 30–32]. Alternatively, charge transfer theories can be used to evaluate rates from quantum chemical calculations [3, 5, 13, 33–35]. In spite of being significantly more computationally demanding, the latter approach allows to link the chemical and electronic structure, as well as the morphology, to charge dynamics.

2.8.1 Classical charge transfer rate

The high temperature limit of classical charge transfer theory [36, 37] is often used as a trade-off between theoretical rigor and computational complexity. It captures key parameters which influence charge transport while at the same time providing an analytical expression for the rate. Within this limit, the transfer rate for a charge to hop from a site i to a site j reads

$$\omega_{ij} = \frac{2\pi}{\hbar} \frac{J_{ij}^2}{\sqrt{4\pi\lambda_{ij}k_{\text{B}}T}} \exp\left[-\frac{(\Delta E_{ij} - \lambda_{ij})^2}{4\lambda_{ij}k_{\text{B}}T}\right], \quad (2.31)$$

where T is the temperature, $\lambda_{ij} = \lambda_{ij}^{\text{int}} + \lambda_{ij}^{\text{out}}$ is the reorganization energy, which is a sum of intra- and inter-molecular (outersphere) contributions, ΔE_{ij} is the site-energy difference, or driving force, and J_{ij} is the electronic coupling element, or transfer integral.

2.8.2 Semi-classical bimolecular rate

The main assumptions in eq. (2.31) are non-adiabaticity (small electronic coupling and charge transfer between two diabatic, non-interacting states), and harmonic promoting modes, which are treated classically. At ambient conditions, however, the intramolecular promoting mode, which roughly corresponds to C-C bond stretching, has a vibrational energy of $\hbar\omega \approx 0.2 \text{ eV} \gg k_{\text{B}}T$ and should be treated quantum-mechanically. The outer-sphere (slow) mode has much lower vibrational energy than the intramolecular promoting mode, and therefore can be treated classically. The weak interaction between molecules also implies that each molecule has its own, practically independent, set of quantum mechanical degrees of freedom.

A more general, quantum-classical expression for a bimolecular multi-channel rate is derived in the Supporting Information of ref. [3] and has the following form

$$\omega_{ij} = \frac{2\pi}{\hbar} \frac{|J_{ij}|^2}{\sqrt{4\pi\lambda_{ij}^{\text{out}}k_{\text{B}}T}} \sum_{l',m'=0}^{\infty} |\langle \chi_{i0}^c | \chi_{il'}^n \rangle|^2 |\langle \chi_{j0}^n | \chi_{jm'}^c \rangle|^2 \exp\left\{-\frac{[\Delta E_{ij} - \hbar(l'\omega_i^n + m'\omega_j^c) - \lambda_{ij}^{\text{out}}]^2}{4\lambda_{ij}^{\text{out}}k_{\text{B}}T}\right\}. \quad (2.32)$$

If the curvatures of intramolecular PES of charged and neutral states of a molecule are different, that is $\omega_i^c \neq \omega_i^n$, the corresponding reorganization energies, $\lambda_i^{cn} = \frac{1}{2}[\omega_i^n(q_i^n - q_i^c)]^2$ and $\lambda_i^{nc} = \frac{1}{2}[\omega_i^c(q_i^n - q_i^c)]^2$, will also differ. In this case the Franck-Condon (FC) factors for discharging of molecule i read [38]

$$|\langle \chi_{i0}^c | \chi_{il'}^n \rangle|^2 = \frac{2}{2^{l'}l'!} \frac{\sqrt{\omega_i^c\omega_i^n}}{(\omega_i^c + \omega_i^n)} \exp(-|s_i|) \left[\sum_{\substack{l'=0 \\ k \text{ even}}}^{l'} \binom{l'}{k} \left(\frac{2\omega_i^c}{\omega_i^c + \omega_i^n}\right)^{k/2} \frac{k!}{(k/2)!} H_{l'-k} \left(\frac{s_i}{\sqrt{2S_i^{cn}}}\right) \right]^2, \quad (2.33)$$

where $H_n(x)$ is a Hermite polynomial, $s_i = 2\sqrt{\lambda_i^{nc}\lambda_i^{cn}}/\hbar(\omega_i^c + \omega_i^n)$, and $S_i^{cn} = \lambda_i^{cn}/\hbar\omega_i^c$. The FC factors for charging of molecule j can be obtained by substituting $(s_i, S_i^{cn}, \omega_i^c)$ with $(-s_j, S_j^{nc}, \omega_j^n)$. In order to evaluate the FC factors, the internal reorganization energy λ_i^{cn} can be computed from the intramolecular PES.

2.8.3 Semi-classical rate

One can also use the quantum-classical rate with a common set of vibrational coordinates [14]

$$\omega_{ij} = \frac{2\pi}{\hbar} \frac{|J_{ij}|^2}{\sqrt{4\pi\lambda_{ij}^{\text{out}}k_{\text{B}}T}} \sum_{N=0}^{\infty} \frac{1}{N!} \left(\frac{\lambda_{ij}^{\text{int}}}{\hbar\omega^{\text{int}}} \right)^N \exp\left(-\frac{\lambda_{ij}^{\text{int}}}{\hbar\omega^{\text{int}}}\right) \exp\left\{-\frac{[\Delta E_{ij} - \hbar N\omega^{\text{int}} - \lambda_{ij}^{\text{out}}]^2}{4\lambda_{ij}^{\text{out}}k_{\text{B}}T}\right\}. \quad (2.34)$$

Numerical estimates show that if $\lambda_{ij}^{\text{int}} \approx \lambda_{ij}^{\text{out}}$ and $|\Delta E_{ij}| \ll \lambda_{ij}^{\text{out}}$ the rates are similar to those of eq. (2.31). In general, there is no robust method to compute $\lambda_{ij}^{\text{out}}$ [39] and both reorganization energies are often assumed to be of the same order of magnitude. In this case the second condition also holds, unless there are large differences in electron affinities or ionization potentials of neighboring molecules, e.g. in donor-acceptor blends.

To calculate rates of the type specified in `options.xml` for all pairs in the `neighbor list` and to save them into the `state.sql` file, run the `rates calculator`. Note that all required ingredients (`reorganization energies`, `transfer integrals`, and `site energies` have to be calculated before).



Calculation of transfer rates

```
! ctp_run -o options.xml -f state.sql -e rates
```

2.9 Master equation

Having determined the list of conjugated segments (hopping sites) and charge transfer rates between them, the next task is to solve the master equation which describes the time evolution of the system

$$\frac{\partial P_{\alpha}}{\partial t} = \sum_{\beta} P_{\beta} \Omega_{\beta\alpha} - \sum_{\beta} P_{\alpha} \Omega_{\alpha\beta}, \quad (2.35)$$

where P_{α} is the probability of the system to be in a state α at time t and $\Omega_{\alpha\beta}$ is the transition rate from state α to state β . A state α is specified by a set of site occupations, $\{\alpha_i\}$, where $\alpha_i = 1(0)$ for an occupied (unoccupied) site i , and the matrix $\hat{\Omega}$ can be constructed from rates ω_{ij} .

The solution of eq. (2.35) is obtained by using kinetic Monte Carlo (KMC) methods. KMC explicitly simulates the dynamics of charge carriers by constructing a Markov chain in state space and can find both stationary and transient solutions of the master equation. The main advantage of KMC is that only states with a direct link to the current state need to be considered at each step. Since these can be constructed solely from current site occupations, extensions to multiple charge carriers (without the mean-field approximation), site-occupation dependent rates (needed for the explicit treatment of Coulomb interactions), and different types of interacting particles and processes, are straightforward. To optimize memory usage and efficiency, a combination of the variable step size method [40] and the first reaction method is implemented.

To obtain the dynamics of charges using KMC, the program `kmc_run` executes a specific `calculator` after reading its options (charge carrier type, runtime, number of carriers etc.) from `options.xml`.



KMC for a single carrier in periodic boundary conditions

```
! kmc_run -o options.xml -f state.sql -e kmcsingle
```



KMC for multiple carriers of the same type in periodic boundary conditions

```
| kmc_run -o options.xml -f state.sql -e kmcmultiple
```

2.9.1 Extrapolation to nondispersive mobilities

Predictions of charge-carrier mobilities in partially disordered semiconductors rely on charge transport simulations in systems which are only several nanometers thick. As a result, simulated charge transport might be dispersive for materials with large energetic disorder [41, 42] and simulated mobilities are system-size dependent. In time-of-flight (TOF) experiments, however, a typical sample thickness is in the micrometer range and transport is often nondispersive. In order to link simulation and experiment, one needs to extract the nondispersive mobility from simulations of small systems, where charge transport is dispersive at room temperature.

Such extrapolation is possible if the temperature dependence of the nondispersive mobility is known in a wide temperature range. For example, one can use analytical results derived for one-dimensional models [43–45]. The mobility-temperature dependence can then be parametrized by simulating charge transport at elevated temperatures, for which transport is nondispersive even for small system sizes. This dependence can then be used to extrapolate to the nondispersive mobility at room temperature [4].

For Alq_3 , the charge carrier mobility of a periodic system of 512 molecules was shown to be more than three orders of magnitude higher than the nondispersive mobility of an infinitely large system [4]. Furthermore, it was shown that the transition between the dispersive and nondispersive transport has a logarithmic dependence on the number of hopping sites N . Hence, a brute-force increase of the system size cannot resolve the problem for compounds with large energetic disorder σ , since N increases exponentially with σ^2 .

2.10 Macroscopic observables

Spatial distributions of charge and current densities can provide a better insight in the microscopic mechanisms of charge transport. If O is an observable which has a value O_α in a state α , its ensemble average at time t is a sum over all states weighted by the probability P_α to be in a state α at time t

$$\langle O \rangle = \sum_{\alpha} O_{\alpha} P_{\alpha}. \quad (2.36) \quad \text{equ:ensemble}$$

If O does not explicitly depend on time, the time evolution of $\langle O \rangle$ can be calculated as

$$\frac{d\langle O \rangle}{dt} = \sum_{\alpha, \beta} [P_{\beta} \Omega_{\beta\alpha} - P_{\alpha} \Omega_{\alpha\beta}] O_{\alpha} = \sum_{\alpha, \beta} P_{\beta} \Omega_{\beta\alpha} [O_{\alpha} - O_{\beta}]. \quad (2.37)$$

If averages are obtained from KMC trajectories, $P_{\alpha} = s_{\alpha}/s$, where s_{α} is the number of Markov chains ending in the state α after time t , and s is the total number of chains.

Alternatively, one can calculate time averages by analyzing a single Markov chain. If the total occupation time of the state α is τ_{α} then

$$\bar{O} = \frac{1}{\tau} \sum_{\alpha} O_{\alpha} \tau_{\alpha}, \quad (2.38) \quad \text{equ:time}$$

where $\tau = \sum_{\alpha} \tau_{\alpha}$ is the total time used for time averaging.

For ergodic systems and sufficient sampling times, ensemble and time averages should give identical results. In many cases, the averaging procedure reflects a specific experimental technique. For example, an ensemble average over several KMC trajectories with different starting conditions corresponds to averaging over injected charge carriers in a time-of-flight experiment. In what follows, we focus on the single charge carrier (low concentration of charges) case.

2.10.1 Charge density

For a specific type of particles, the microscopic charge density of a site i is proportional to the occupation probability of the site, p_i

$$\rho_i = ep_i/V_i, \quad (2.39)$$

where, for an irregular lattice, the effective volume V_i can be obtained from a Voronoi tessellation of space. For reasonably uniform lattices (uniform site densities) this volume is almost independent of the site and a constant volume per site, $V_i = V/N$, can be assumed. In the macroscopic limit, the charge density can be calculated using a smoothing kernel function, i.e. a distance-weighted average over multiple sites. Site occupations p_i can be obtained from eq. (2.36) or eq. (2.38) by using the occupation of site i in state α as an observable.

If the system is in thermodynamic equilibrium, that is without sources or sinks and without circular currents (and therefore no net flux) a condition, known as detailed balance, holds

$$p_j\omega_{ji} = p_i\omega_{ij}, \quad (2.40)$$

It can be used to test whether the system is ergodic or not by correlating $\log p_i$ and the site energy E_i . Indeed, if $\lambda_{ij} = \lambda_{ji}$ the ratios of forward and backward rates are determined solely by the energetic disorder, $\omega_{ji}/\omega_{ij} = \exp(-\Delta E_{ij}/k_B T)$ (see eq. (2.31)).

2.10.2 Current

If the position of the charge, \vec{r} , is an observable, the time evolution of its average $\langle \vec{r} \rangle$ is the total current in the system

$$\vec{J} = e \langle \dot{\vec{r}} \rangle = e \frac{d \langle \vec{r} \rangle}{dt} = e \sum_{i,j} p_j \omega_{ji} (\vec{r}_i - \vec{r}_j). \quad (2.41)$$

Symmetrizing this expression we obtain

$$\vec{J} = \frac{1}{2} e \sum_{i,j} (p_j \omega_{ji} - p_i \omega_{ij}) \vec{r}_{ij}, \quad (2.42)$$

where $\vec{r}_{ij} = \vec{r}_i - \vec{r}_j$. Symmetrization ensures equal flux splitting between neighboring sites and absence of local average fluxes in equilibrium. It allows to define a local current through site i as

$$\vec{J}_i = \frac{1}{2} e \sum_j (p_j \omega_{ji} - p_i \omega_{ij}) \vec{r}_{ij}. \quad (2.43)$$

A large value of the local current indicates that the site contributes considerably to the total current. A collection of such sites thus represents most favorable charge pathways [46].

2.10.3 Mobility and diffusion constant

For a single particle, e.g. a charge or an exciton, a zero-field mobility can be determined by studying particle diffusion in the absence of external fields. Using the particle displacement squared, Δr_i^2 , as an observable we obtain

$$2dD_{\gamma\delta} = \frac{d \langle \Delta r_{i,\gamma} \Delta r_{i,\delta} \rangle}{dt} = \sum_{\substack{i,j \\ i \neq j}} p_j \omega_{ji} (\Delta r_{i,\gamma} \Delta r_{i,\delta} - \Delta r_{j,\gamma} \Delta r_{j,\delta}) = \sum_{\substack{i,j \\ i \neq j}} p_j \omega_{ji} (r_{i,\gamma} r_{i,\delta} - r_{j,\gamma} r_{j,\delta}). \quad (2.44)$$

Here \vec{r}_i is the coordinate of the site i , $D_{\gamma\delta}$ is the diffusion tensor, $\gamma, \delta = x, y, z$, and $d = 3$ is the system dimension. Using the Einstein relation,

$$D_{\gamma\delta} = k_B T \mu_{\gamma\delta}, \quad (2.45)$$

one can, in principle, obtain the zero-field mobility tensor $\mu_{\gamma\delta}$. Eq. (2.44), however, does not take into account the use of periodic boundary conditions when simulating charge dynamics. In this case, the simulated occupation probabilities can be compared to the solution of the Smoluchowski equation with periodic boundary conditions (see the supporting information for details).

Alternatively, one can directly analyze time-evolution of the KMC trajectory and obtain the diffusion tensor from a linear fit to the mean square displacement, $\overline{\Delta r_{i,\gamma} \Delta r_{i,\delta}} = 2dD_{\gamma\delta}t$.

The charge carrier mobility tensor, $\hat{\mu}$, for any value of the external field can be determined either from the average charge velocity defined in eq. (2.41)

$$\langle \vec{v} \rangle = \sum_{i,j} p_j \omega_{ji} (\vec{r}_i - \vec{r}_j) = \hat{\mu} \vec{F}, \quad (2.46)$$

or directly from the KMC trajectory. In the latter case the velocity is calculated from the unwrapped (if periodic boundary conditions are used) charge displacement vector divided by the total simulation time. Projecting this velocity on the direction of the field \vec{F} yields the charge carrier mobility in this particular direction. In order to improve statistics, mobilities can be averaged over several KMC trajectories and MD snapshots.

2.10.4 Spatial correlations of energetic disorder

Long-range, e.g. electrostatic and polarization, interactions often result in spatially correlated disorder [47], which affects the onset of the mobility-field (Poole-Frenkel) dependence [43, 48, 49]. To quantify the degree of correlation, one can calculate the spatial correlation function of E_i and E_j at a distance r_{ij}

$$C(r_{ij}) = \frac{\langle (E_i - \langle E \rangle) (E_j - \langle E \rangle) \rangle}{\langle (E_i - \langle E \rangle)^2 \rangle}, \quad (2.47)$$

where $\langle E \rangle$ is the average site energy. $C(r_{ij})$ is zero if E_i and E_j are uncorrelated and 1 if they are fully correlated. For a system of randomly oriented point dipoles, the correlation function decays as $1/r$ at large distances [50].

For systems with spatial correlations, variations in site energy differences, ΔE_{ij} , of pairs of molecules from the neighbor list are smaller than variations in site energies, E_i , of all individual molecules. Since only neighbor list pairs affect transport, the distribution of ΔE_{ij} rather than that of individual site energies, E_i , should be used to characterize energetic disorder.

Note that the `eanalyze` calculator takes into account *all* contributions to the site energies



Analyze distribution and correlations of site energies

```
| ctp_run -o options.xml -f state.sql -e eanalyze
```

2.10.5 DFT-based transfer integrals using DIPRO

The calculation of one electronic coupling element based on DFT using the DIPRO method requires the overlap matrix of atomic orbitals \mathcal{S} , the expansion coefficients for monomer $\bar{\lambda}_{(k)} = \{\lambda_{\alpha}^{(k)}\}$ and dimer orbitals $\bar{\mathbf{D}}_{(n)} = \{D_{\alpha}^{(n)}\}$, as well as the orbital energies E_n of the dimer are required as input. In practical situations, performing self-consistent quantum-chemical calculations for each individual monomer and one for the dimer to obtain this input data is extremely demanding. Several simplifications can be made to reduce the computational effort, such as using non-Counterpoise basis sets for the monomers (thereby decoupling the monomer calculations from the dimer run) and performing only a single SCF step in a dimer calculation starting from an initial guess formed from a superposition of monomer orbitals. This "noCP+noSCF" variant of DIPRO is shown in figure 2.4(a) and recommended for production runs. A detailed comparative study of the different variants can be found in [5].

814 The code currently contains supports evaluation of transfer integrals from quantum-chemical
 815 calculations performed with the Gaussian, Turbomole, and NWChem packages. The interfac-
 816 ing procedure consists of three main steps: generation of input files for monomers and dimers,
 817 performing the actual quantum-chemical calculations, and calculating the transfer integrals.

818 Monomer calculations

sec:edft

819 First, **hopping sites** and a **neighbor list** need to be generated from the atomistic topology and
 820 trajectory and written to the `state.sql` file. Then the parallel **edft calculator** manages the
 821 calculation of the monomer properties required for the determination of electronic coupling ele-
 822 ments. Specifically, the individual steps it performs are:

- 823 1. Creation of a job file containing the list of molecules to be calculated with DFT

Writing job file for **edft**

```
| ctp_parallel -o options.xml -f state.sql -e edft -j write
```

- 824 2. Running of all jobs in job file

Running all **edft** jobs

```
| ctp_parallel -o options.xml -f state.sql -e edft -j run
```

825 which includes

- 826 • creating the input files for the DFT calculation (using the package specified in `options.xml`)
 827 in the directory

828 `OR_FILES/package/frame_F/mol_M`

829 where `F` is the index of the frame in the trajectory, `M` is the index of a molecule in this
 830 frame,

- 831 • executing the DFT run, and
- 832 • after completion of this run, parsing the output (number of electrons, basis set, molec-
 833 ular orbital expansion coefficients), and saving it in compressed form to

834 `OR_FILES/molecules/frame_F/molecule_M.orb`

835 Calculating the transfer integrals

sec:edft


836 After the monomer calculations have been completed successfully, the respective runs for dimers
 837 from the neighborlist can be performed using the parallel **idft calculator**, which manages the
 838 DFT runs for the hopping pairs and determines the coupling element using DIPRO. Again, sev-
 839 eral steps are required:

- 840 1. Creation of a job file containing the list of pairs to be calculated with DFT

Writing job file for **idft**

```
| ctp_parallel -o options.xml -f state.sql -e idft -j write
```

- 841 2. Running of all jobs in job file

 **Running all `idft` jobs**

```
| ctp_parallel -o options.xml -f state.sql -e idft -j run
```

842 which includes

- 843
- 844 • creating the input files (including the merged guess for a noSCF calculation, if re-
 - 845 requested) for the DFT calculation (using the package specified in `options.xml`) in the

846 `OR_FILES/package/frame_F/pair_M_N`

847 where M and N are the indices of the molecules in this pair,

- 848
- 849 • executing the DFT run, and
 - 850 • after completion of this run, parsing the output (number of electrons, basis set, molec-
 - 851 ular orbital expansion coefficients and energies, atomic orbital overlap matrix), and


852 `OR_FILES/pairs/frame_F/pair_M_N.orb`

- 853
- 854 • loading the monomer orbitals from the previously saved `*.orb` files.

- 854 • calculating the coupling elements and write them to the job file

855 3. Reading the coupling elements from the job file and saving them to the `state.sql` file

856

 **Saving `idft` results from job file to `state.sql`**

```
| ctp_parallel -o options.xml -f state.sql -e idft -j read
```

Chapter 3

Input and output files

3.1 Atomistic topology

If you are using GROMACS for generating atomistic configurations, it is possible to directly use the topology file provided by GROMACS (`topology.tpr`). In this case the GROMACS residue and atom names should be used to specify the coarse-grained topology and conjugated segments. A custom topology can also be defined using an XML file. Moreover, it is possible to partially overwrite the information provided in, for example, GROMACS topology file. We will illustrate how to create a custom topology file using DCV2T. The structure of DCV2T, together with atom type definitions, is shown in fig. 3.1. DCV2T has two thiophene (THI) and two dicyanovinyl (NIT) residues. The pdb file which contains residue types, residue numbering, atom names, atom types, and atom coordinates is shown in listing 3.1.

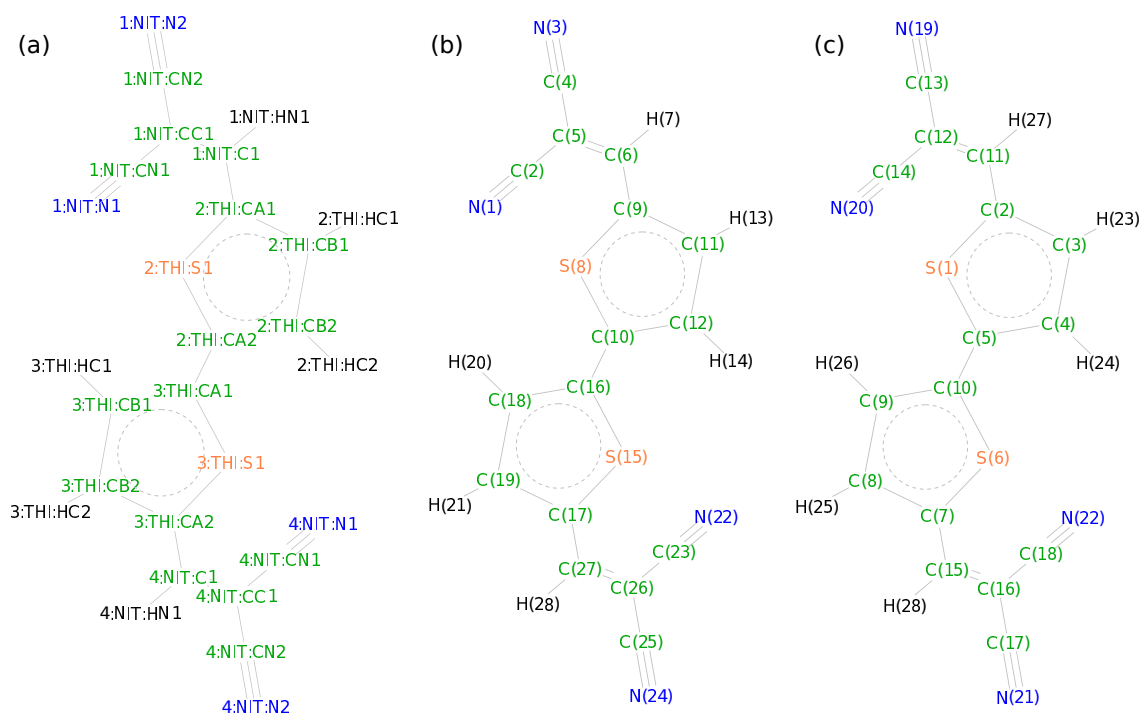


Figure 3.1: (a) DCV2T with atoms labelled according to `residue_number:residue_name:atom_name`. There are four residues and two residue types: thiophene (THI) and dicyanovinyl (NIT). The corresponding pdb file is shown in listing 3.1. Atom numbering is used to split conjugated segments on rigid fragments and to link atomistic (b) from GROMACS topology) and quantum descriptions (c).

fig:dcv2t

list.pdb

Listing 3.1: pdb file of DCV2T.

869											
870	HETATM	1	N1	NIT	1	2.388	8.533	11.066	1.00	4.14	N
871	HETATM	2	CN1	NIT	1	1.984	9.553	10.718	1.00	2.54	C
872	HETATM	3	N2	NIT	1	-1.138	10.872	10.087	1.00	3.24	N
873	HETATM	4	CN2	NIT	1	0.003	10.871	10.213	1.00	2.37	C
874	HETATM	5	CC1	NIT	1	1.441	10.824	10.327	1.00	1.91	C
875	HETATM	6	C1	NIT	1	2.193	11.939	10.071	1.00	1.61	C
876	HETATM	7	HN1	NIT	1	1.715	12.710	9.872	1.00	1.97	H
877	HETATM	8	S1	THI	2	4.758	10.743	10.130	1.00	1.52	S
878	HETATM	9	CA1	THI	2	3.613	12.024	9.948	1.00	1.22	C
879	HETATM	10	CA2	THI	2	6.099	11.836	9.997	1.00	1.30	C
880	HETATM	11	CB1	THI	2	4.251	13.243	9.782	1.00	1.39	C
881	HETATM	12	CB2	THI	2	5.658	13.131	9.818	1.00	1.45	C
882	HETATM	13	HC1	THI	2	3.800	14.047	9.660	1.00	1.66	H
883	HETATM	14	HC2	THI	2	6.230	13.860	9.731	1.00	1.74	H
884	HETATM	15	S1	THI	3	8.803	12.414	9.882	1.00	1.38	S
885	HETATM	16	CA1	THI	3	7.456	11.347	10.094	1.00	1.37	C
886	HETATM	17	CA2	THI	3	9.940	11.122	10.152	1.00	1.42	C
887	HETATM	18	CB1	THI	3	7.873	10.048	10.355	1.00	1.73	C
888	HETATM	19	CB2	THI	3	9.267	9.926	10.399	1.00	1.82	C
889	HETATM	20	HC1	THI	3	7.288	9.335	10.487	1.00	2.05	H
890	HETATM	21	HC2	THI	3	9.704	9.123	10.576	1.00	2.21	H
891	HETATM	22	N1	NIT	4	11.235	14.572	9.094	1.00	3.08	N
892	HETATM	23	CN1	NIT	4	11.665	13.566	9.441	1.00	2.04	C
893	HETATM	24	N2	NIT	4	14.733	12.005	10.009	1.00	2.17	N
894	HETATM	25	CN2	NIT	4	13.590	12.149	9.933	1.00	1.77	C
895	HETATM	26	CC1	NIT	4	12.156	12.282	9.861	1.00	1.71	C
896	HETATM	27	C1	NIT	4	11.363	11.220	10.154	1.00	1.59	C
897	HETATM	28	HN1	NIT	4	11.813	10.440	10.389	1.00	1.89	H

3.2 Mapping file

899

sec.xmlmap

The mapping file (referred here as `map.xml`) is used by the program `ctp_map` to convert an atomistic trajectory to a trajectory with conjugated segments and rigid fragments. This trajectory is stored in a state file and contains positions, names, types of atoms belonging to rigid fragments. The description of the mapping options is given in table 3.1. An example of `map.xml` for a DCV2T molecule is shown in listing 3.2.

The file `map.xml` contains the whole electrostatic information about the molecules as well as the structural information. The `toolpdb2map` creates a `map.xml` from a `pdb` file and is a good starting point for further refinement.

tab.map

Table 3.1: Description of the XML mapping file (`map.xml`).

907

list.map

Listing 3.2: Examl of `map.xml` for DCV2T. Each rigid fragment (coarse-grained bead) is defined by a list of atoms. Atom numbers, names, and residue names should correspond to those used in GROMACS topology (see the corresponding listing 3.1 of the `pdb` file).

```

908 <!-- this file is used to conver an atomistic trajectory to conjugated segments -->
909 <!-- name of the conjugated molecule -->
910 <!-- corresponding name of this molecule in the MD trajectory, should be
911 the same as the name given at the end of topol.top -->
912 <!-- name of the conjugated segment within the molecule -->
913 <!-- QM coordinates of the conjugated segment -->
914 <!-- IZINDO INPUT -->
915 <!-- name of the conjugated segment within the molecule -->
916 <!-- QM coordinates of the conjugated segment -->
917 <!-- EMULTIPOLE INPUT -->
918 <!-- Multipole file for neutral state -->
919 <!-- Multipole file for hole state -->
920 <!-- specifies if planar QM coordinates (map2md=0) or MD coordinates (
921 map2md=1) of atoms are used for distribution of partial charges. For MD coordinates the
922 order and numbering in <mdatoms> and <mipoles> must be identical it has no impact on the
923 qm e.g. DFT or GWBSE calculations -->
924 <!-- EINTERNAL INPUT -->
925 <!-- Site energy -->
926 <!-- Reorg. discharge -->
927 <!-- Reorg. charge -->
928 <!-- MD QM MP Mapping -->
929 <!-- name of the rigid fragment within the segment -->
930 <!-- list of atoms in the fragment resnum:resname:atomname -->
931 <!-- corresponding ground state geometry atomnumber:atomtype read from .xyz file -->
932 <!-- corresponding group state geometry multipoles read from .mps files -->
933 <!-- weights to determine the fragment center (here CoM is used) -->
934 <!-- three atoms: define a cartesian local frame, two atoms: fragment is assumed to be
935 rotationally invariant around the axis, one atom: fragment is assumed isotropic -->
936 <!-- Optional parameters (if not set <localframe> is used): used when atom labels in the .mps
937 and .xyz file differ or more sites in the .mps file are used, so refers to <mipoles> -->
938 <!-- Optional parameters (if not set <localframe> is used): weights to determine the
939 fragment center (here CoM is used), used when atom labels in the .mps and .xyz file
940 differ or additional sites in the .mps file are used -->
941 <!-- Optional flag: says if a site is virtual or not, (virtual=1, real=0) -->

```

```

963     <virtual_mps> 0 0 0 0 0 0 0 0 </
964     virtual_mps>
965 </fragment>
966
967 <fragment>
968   <name>TH1</name>
969   <mdatoms>2:THI:S1 2:THI:CA1 2:THI:CA2 2:THI:CB1 2:THI:CB2 2:THI:HC1 2:THI:HC2</mdatoms>
970   <qmatoms> 7:S 8:C 6:C 9:C 10:C 24:H 25:H </qmatoms>
971   <mpoles> 7:S 8:C 6:C 9:C 10:C 24:H 25:H </mpoles>
972   <weights> 32 12 12 12 12 1 1 </weights>
973   <localframe> 7 8 6 </localframe>
974 </fragment>
975
976 <fragment>
977   <name>TH2</name>
978   <mdatoms>3:THI:S1 3:THI:CA1 3:THI:CA2 3:THI:CB1 3:THI:CB2 3:THI:HC1 3:THI:HC2</mdatoms>
979   <qmatoms> 3:S 4:C 2:C 5:C 1:C 26:H 27:H </qmatoms>
980   <weights> 32 12 12 12 12 1 1 </weights>
981   <localframe> 3 4 2 </localframe>
982 </fragment>
983
984 <fragment>
985   <name>NI2</name>
986   <mdatoms>4:NIT:N1 4:NIT:CN1 4:NIT:N2 4:NIT:CN2 4:NIT:CC1 4:NIT:C1 4:NIT:HN1</mdatoms>
987   <qmatoms> 22:N 21:C 18:N 17:C 16:C 15:C 28:H </qmatoms>
988   <mpoles> 22:N 21:C 18:N 17:C 16:C 15:C 28:H </mpoles>
989   <weights> 14 12 14 12 12 12 1 </weights>
990   <localframe> 22 21 18 </localframe>
991 </fragment>
992 </fragments>
993 </segment>
994 </segments>
995 </molecule>
996 </molecules>
997 </topology>

```

3.3 Conjugated segments

The file describing hopping sites, or conjugated segments, is used by practically all programs and calculators. It links the coarse-grained trajectory (positions and orientations of rigid fragments) and quantum-mechanical descriptions of all conjugated segments. The description of this XML file (`segments.xml`) is given in table 3.2. An example for DCV2T is shown in listing 3.3.

Table 3.2: Description of conjugated segments (`segments.xml`).

Listing 3.3: XML file describing conjugated segments. Note that the mapping and weights for each segment are separated by a colon.

```

1004 <segments>
1005   <segment> <!-- DCV2T here is one conjugated segment -->
1006     <coordinates>DCV2T.xyz</coordinates> <!-- xyz coordinates -->
1007     <orbitals>DCV2T.fort.7</orbitals> <!-- ZINDO orbitals [GAUSSIAN] -->
1008     <basisset>INDO</basisset>
1009     <torbital>50</torbital> <!-- HOMO for hole conduction -->
1010     <edischarging>0.084</edischarging> <!-- reorganization energy -->
1011     <echarging>0.086</echarging> <!-- reorganization energy -->
1012     <qneutral>DCV2T_neutr.esp</qneutral> <!-- partial charges of a neutral molecule -->
1013     <qcharged>DCV2T_catio.esp</qcharged> <!-- partial charges of a cation -->
1014     <energy>0.0</energy> <!-- cite energy -->
1015     <name>DCV2T</name> <!-- name of the conjugated segment -->
1016     <map> <!-- rigid fragments separated by a colon -->
1017       22 21 18 17 16 15 28:
1018       3 2 4 1 5 27 26:
1019       7 6 8 10 9 25 24:
1020       20 19 14 13 12 11 23
1021     </map>
1022     <weights> <!-- for centers of rigid fragments -->
1023       14 12 14 12 12 12 1:
1024       32 12 12 12 12 1 1:
1025       32 12 12 12 12 1 1:
1026       14 12 14 12 12 12 1
1027

```

```

1028         </weights>
1029     </segment>
1030 </segments>

```

3.4 Molecular orbitals

If the semi-empirical method is used to calculate electronic coupling elements, molecular orbitals of all molecules must be supplied. They can be generated using Gaussian program. The Gaussian input file for DCV2T is shown in listing 3.4. Provided with this input, Gaussian will generate `fort.7` file which contains the molecular orbitals of a DCV2T. This file can be renamed to `DCV2T.orb`. Note that the order of the atoms in the input file and the order of coefficients should always match. Therefore, the coordinate part of the input file must be supplied together with the orbitals. We will assume the coordinates, in the format `atom_type: x y z`, is saved to the `DCV2T.xyz` file.

Attention

Izindo requires the specification of orbitals for hole and electron transport in `map.xml`. They are the HOMO and LUMO respectively and can be retrieved from the `log` file from which the `DCV2T.orb` file is generated. The number of alpha electrons is the HOMO, the LUMO is HOMO+1

`list:zindo_orbitals`

Listing 3.4: Gaussian input file `get_orbitals.com` used for generating molecular orbitals. The first line contains the name of the check file, the second the requested RAM. `int=zindos` requests the method ZINDO, `punch=mo` states that the molecular orbitals ought to be written to the `fort.7` file, `nosymm` forbids use of symmetry and is necessary to ensure correct position of orbitals with respect to the provided coordinates. The two integer numbers correspond to the charge and multiplicity of the system: 0 1 corresponds to a neutral system with a multiplicity of one. They are followed by the types and coordinates of all atoms in the molecule.

```

1041
1042 %chk=DCV2T.chk
1043 %mem=100Mb
1044 #p int=zindos punch=mo nosymm
1045
1046 DCV2T molecular orbitals
1047
1048 0 1
1049 S      -1.44650      2.12185      0.00135
1050 C      -2.43098      0.58936     -0.00048
1051 C      -1.59065     -0.51859     -0.00146
1052 C      -0.21222     -0.22233     -0.00095
1053 C      0.07761      1.13376      0.00040
1054 S      2.87651      0.79316      0.00148
1055 C      3.86099      2.32565      0.00235
1056 C      3.02066      3.43359      0.00231
1057 C      1.64223      3.13733      0.00162
1058 C      1.35240      1.78125      0.00114
1059 C      -3.85350      0.52245     -0.00081
1060 C      -4.79569      1.52479     -0.00008
1061 C      -6.18500      1.18622     -0.00117
1062 C      -4.47544      2.91565      0.00081
1063 C      5.28350      2.39256      0.00296
1064 C      6.22569      1.39020      0.00327
1065 C      7.61500      1.72876      0.00432
1066 C      5.90542     -0.00064      0.00333
1067 N      -7.32389      0.89743     -0.00195
1068 N      -4.21872      4.06274      0.00142
1069 N      8.75389      2.01754      0.00510
1070 N      5.64864     -1.14772      0.00361
1071 H      -1.98064     -1.52966     -0.00256
1072 H      0.55785     -0.98374     -0.00169

```

1073	H	3.41065	4.44466	0.00272
1074	H	0.87216	3.89874	0.00147
1075	H	-4.24640	-0.49192	-0.00188
1079	H	5.67641	3.40692	0.00337

1078 3.5 Monomer calculations for DFT transfer integrals

list.edft_gaussian.xml

Listing 3.5: Example `package.xml` file for the Gaussian package required in the options of the `edft calculator` for the monomer calculations as preparation for the determination of transfer integrals using DIPRO.

```

1079 <package>
1080   <name>gaussian</name>
1081   <executable>g09</executable>
1082   <checkpoint></checkpoint>
1083   <scratch></scratch>
1084
1085   <charge>0</charge>
1086   <spin>1</spin>
1087   <options># pop=minimal pbepbe/6-311g** scf=tight punch=mo nosymm test</options>
1088   <memory>1Gb</memory>
1089   <threads>2</threads>
1090
1091   <cleanup></cleanup>
1092 </package>
1093

```

list.edft_turbomole.xml

Listing 3.6: Example `package.xml` file for the Turbomole package required in the options of the `edft calculator` for the monomer calculations as preparation for the determination of transfer integrals using DIPRO.

```

1095 <package>
1096   <name>turbomole</name>
1097   <executable>ridft</executable>
1098   <scratch>/tmp</scratch>
1099
1100   <options>
1101     TITLE
1102     a coord
1103     *
1104     no
1105     b all def-TZVP
1106     *
1107     eht
1108     y
1109     0
1110     y
1111     dft
1112     on
1113     func
1114     pbe
1115     grid
1116     m3
1117     *
1118     ri
1119     on
1120     m 300
1121     *
1122     scf
1123     conv
1124     7
1125     iter
1126     200
1127
1128

```



```

1129 marij
1130
1131 q
1132   </options>
1133
1134   <cleanup></cleanup>
1135 </package>

```

list:edft_nwchem.xml

Listing 3.7: Example `package.xml` file for the NWChem package required in the options of the `edft` calculator for the monomer calculations as preparation for the determination of transfer integrals using DIPRO.

```

1137
1138 <package>
1139   <name>nwchem</name>
1140   <executable>nwchem</executable>
1141   <checkpoint></checkpoint>
1142   <scratch>/tmp/nwchem</scratch>
1143   <charge>0</charge>
1144   <spin>1</spin>
1145   <threads>1</threads>
1146   <memory></memory>
1147   <options>
1148     start
1149     basis
1150       * library 6-311gss
1151     end
1152     memory 1500 mb
1153
1154     dft
1155       xc xpbe96 cpbe96
1156       direct
1157       iterations 100
1158       noprint "final vectors analysis"
1159     end
1160     task dft
1161   </options>
1162   <cleanup></cleanup>
1163 </package>

```

3.6 Pair calculations for DFT transfer integrals

list:idft_gaussian.xml

Listing 3.8: Example `package.xml` file for the Gaussian package required in the options of the `idft` calculator for the pair calculations and the determination of transfer integrals using DIPRO.

```

1166
1167 <package>
1168   <name>gaussian</name>
1169   <executable>g09</executable>
1170   <checkpoint></checkpoint>
1171   <scratch></scratch>
1172
1173   <charge>0</charge>
1174   <spin>1</spin>
1175   <options># pop=minimal pbepbe/6-311g** nosymm IOp(3/33=1,3/36=-1) punch=mo guess=cards scf=(maxcycle=1,
1176   <memory>1Gb</memory>
1177   <threads>1</threads>
1178
1179   <cleanup></cleanup>
1180 </package>

```

list:idft_turbomole.xml

Listing 3.9: Example `package.xml` file for the Turbomole package required in the options of the `idft` calculator for the pair calculations and the determination of transfer integrals using DIPRO.

```

1182 <package>
1183

```

```

1184 <name>turbomole</name>
1185 <executable>ridft</executable>
1186 <scratch>/tmp</scratch>
1187
1188 <options>
1189 $intsdebug cao
1190 a coord
1191 *
1192 no
1193 b all def-TZVP
1194 *
1195 eht
1196 y
1197 0
1198 y
1199 dft
1200 on
1201 func
1202 pbe
1203 grid
1204 m3
1205 *
1206 ri
1207 on
1208 m 300
1209 *
1210 scf
1211 conv
1212 7
1213 iter
1214 1
1215 diis
1216 3
1217 damp
1218 0.00
1219
1220
1221
1222 marij
1223
1224 q
1225 </options>
1226
1227 <cleanup></cleanup>
1228 </package>

```

list.idft_nwchem.xml

Listing 3.10: Example package.xml file for the NWChem package required in the options of the `idft` calculator for the pair calculations and the determination of transfer integrals using DIPRO.

```

1230
1231 <package>
1232 <name>nwchem</name>
1233 <executable>nwchem</executable>
1234 <checkpoint></checkpoint>
1235 <scratch>/tmp/nwchem</scratch>
1236 <charge>0</charge>
1237 <spin>1</spin>
1238 <memory></memory>
1239 <threads>1</threads>
1240 <options>
1241 start
1242 basis
1243 * library 6-311gss
1244 end
1245 memory 1500 mb
1246
1247 dft
1248 print "ao overlap"

```

```

1249 xc xpbe96 cpbe96
1250 direct
1251 iterations 1
1252 convergence nodamping nodiis
1253 noprint "final vectors analysis"
1254 vectors input system.movecs
1255 end
1256 task dft
1257 </options>
1258 <cleanup></cleanup>
1259 </package>

```

3.7 DFT transfer integrals

list:TI.xml

Listing 3.11: Example TI.xml file created as the output of a DIPRO calculation. Due to slightly different implementations, the orbitals indices refer to monomer indices in a Gaussian run but to indices in the merged dimer guess in a Turbomole run.

```

1262
1263 <pair name="pair_100_155">
1264   <parameters>
1265     <HOMO_A>162</HOMO_A>
1266     <NoccA>1</NoccA>
1267     <LUMO_A>164</LUMO_A>
1268     <NvirtA>1</NvirtA>
1269     <HOMO_B>161</HOMO_B>
1270     <NoccB>1</NoccB>
1271     <LUMO_B>163</LUMO_B>
1272     <NvirtB>1</NvirtB>
1273   </parameters>
1274   <transport name="hole">
1275     <channel name="single">
1276       <J>1.546400416750696E-003</J>
1277       <e_A>-6.30726450715697</e_A>
1278       <e_B>-6.36775613794166</e_B>
1279     </channel>
1280     <channel name="multi">
1281       <molecule name="A">
1282         <e_HOMOm0>-6.30726450715697</e_HOMOm0>
1283       </molecule>
1284       <molecule name="B">
1285         <e_HOMOm0>-6.36775613794166</e_HOMOm0>
1286       </molecule>
1287       <dimer name="integrals">
1288         <T_00>1.546400416750696E-003</T_00>
1289         <J_sq_degen>2.391354248926727E-006</J_sq_degen>
1290         <J_sq_boltz>2.391354248926727E-006</J_sq_boltz>
1291       </dimer>
1292     </channel>
1293   </transport>
1294   <transport name="electron">
1295     <channel name="single">
1296       <J>-2.797473760331286E-003</J>
1297       <e_A>-4.50318366770689</e_A>
1298       <e_B>-4.53143397059021</e_B>
1299     </channel>
1300     <channel name="multi">
1301       <molecule name="A">
1302         <e_LUMOp0>-4.50318366770689</e_LUMOp0>
1303       </molecule>
1304       <molecule name="B">
1305         <e_LUMOp0>-4.53143397059021</e_LUMOp0>
1306       </molecule>
1307       <dimer name="integrals">
1308         <T_00>-2.797473760331286E-003</T_00>

```

```

1309         <J_sq_degen>7.825859439742066E-006</J_sq_degen>
1310         <J_sq_boltz>7.825859439742066E-006</J_sq_boltz>
1311     </dimer>
1312 </channel>
1313 </transport>
1314 </pair>

```

1316 3.8 State file

sec.statefile

1317 All data structures are saved to the `state.sql` file in sqlite3 format, see <http://www.sqlite.org/>.
1318 They are available in form of tables in the `state.sql` file as can be seen by the command
1319 `sqlite3 state.sql ".tables "`
1320 An example of such a table are molecules. The full table can be displayed using the command
1321 (similar for the other tables)
1322 `sqlite3 state.sql " SELECT * FROM molecules "`
1323 The meaning of all the entries in the table can be displayed by a command like
1324 `sqlite3 state.sql ".SCHEMA molecules "`
1325 The first and second entry are integers for internal and regular id of the molecule and the third
1326 entry is the name. A single field from the table like the name of the molecule can be displayed by
1327 a command like
1328 `sqlite3 state.sql " SELECT name FROM molecules "`
1329 Besides molecules, the following tables are stored in the `state.sql`:
1330 `conjseg_properties`:
1331 Conjugated segments are stored with id, name and x,y,z coordinates of the center of mass in nm.
1332 `conjsegs`:
1333 Reorganization energies for charging or discharging a conjugated segment are stored together
1334 with the coulomb energy and any other user defined energy contribution (in eV) and occupation
1335 probabilities.
1336 `pairs`:
1337 The pairs from the neighborlist are stored with the pair id, the id of the first and second segment,
1338 the rate from the first to the second , the rate from the second to the first (both in s⁻¹) and the
1339 x,y,z coordinates in nm of the distance between the first and the second segment.
1340 `pairintegrals`:
1341 Transfer integrals for all pairs are stored in the following way: The pair id , the number for count-
1342 ing possible different electronic overlaps (e.g if only the frontier orbitals are taken into account
1343 this is always zero, while an effective value is stored in addition to the different overlaps of e.g.
1344 HOMO-1 and HOMO-1 if more frontier orbitals are taken into account) and the integral in eV.
1345 `pairproperties`:
1346 The outer sphere reorganization energy of all pairs is stored by an id, the pair id, a string `lambda_outer`
1347 and the energy in eV.
1348 `conjsegs`:
1349 Conjugated segments are saved in the following way: The id, the name, the type, the molecule
1350 id, the time frame, the x,y,z coordinates in nm and the occupation probability.
1351 `conjseg_properties`:
1352 Properties of the conjugated segments like reorganization energies for charging or discharging a
1353 charge unit or the coulomb contribution to the site energy are stored by: id, conjugated segment
1354 id, a string like `lambda_intra_charging`, `lambda_intra_discharging` or `energy_coulomb`
1355 and a corresponding value in eV.
1356 The tables `rigidfrag_properties`, `rigidfrags` and `frames` offer information about rigid
1357 fragments and time frames including periodic boundary conditions.
1358 The data in the `state.sql` file can also be modified by the user. Here is an example how to
1359 modify the transfer integral between the conjugated segments number one and two assuming
1360 that they are in the neighborlist. Their pair id can be found by the command

```
1361 pair_ID=`sqlite3 state.sql "SELECT _id FROM pairs WHERE conjseg1=1 AND conjseg2=2" `
1362 The old value of the transfer integral can be deleted using
1363 sqlite3 state.sql "DELETE FROM pair_integrals WHERE pair=$pair_ID"
1364 Finally the new transfer integral  $J$  can be written to the state.sql file by the command
1365 sqlite3 state.sql "INSERT INTO pair_integrals (pair,num,J) VALUES ($pair_ID,0,$J) "
1366 Here the num=0 indicates that only the effective transfer integrals is written to the file, while other
1367 values of num would correspond to overlap between other orbitals than the frontier orbitals.
1368 In a similar way the coulomb contribution to the site energy of the first conjugated segment can
1369 be overwritten by first getting its id
1370 c_ID=`sqlite3 state.sql "SELECT _id from conjseg_properties where conjseg=1 AND
1371 key =\"energy_coulomb\""
1372 Then deleting the old value
1373 sqlite3 state.sql "DELETE FROM from conjseg_properties WHERE _id=$c_ID"
1374 Then the new coulomb energy  $E$  can be written to this id
1375 sqlite3 state.sql "INSERT INTO conjseg_properties (_id,conjseg,key,value)
1376 VALUES ($c_ID,1,\"energy_coulomb\",$E) "
1377 Finally the resulting coulomb contribution to all conjugated segments can be displayed by
1378 sqlite3 state.sql "SELECT * from conjseg_properties WHERE key=\"energy_coulomb\""
1379
```


1380 Chapter 4

1381 Reference

sec:reference

1382 4.1 Programs

sec:programs

1383 Programs execute specific tasks (calculators).

1384 4.1.1 ctp_map

prog:ctp_map

1385 Generates QM | MD topology

1386 -h [--help] display this help and exit
1387 -v [--verbose] be loud and noisy
1388 -t [--topology] arg topology
1389 -c [--coordinates] arg coordinates or trajectory
1390 -s [--segments] arg definition of segments and fragments
1391 -f [--file] arg state file
1392 --man output man-formatted manual pages
1393 --tex output tex-formatted manual pages

1394 4.1.2 ctp_dump

prog:ctp_dump

1395 Extracts information from the state file

1396 -h [--help] display this help and exit
1397 -v [--verbose] be loud and noisy
1398 -o [--options] arg calculator options
1399 -f [--file] arg sqlight state file, *.sql
1400 -i [--first-frame] arg (=1) start from this frame
1401 -n [--nframes] arg (=1) number of frames to process
1402 -t [--nthreads] arg (=1) number of threads to create
1403 -s [--save] arg (=1) whether or not to save changes to state file
1404 -e [--extract] arg List of extractors separated by ',' or ''
1405 -l [--list] Lists all available extractors
1406 -d [--description] arg Short description of an extractor
1407 --man output man-formatted manual pages
1408 --tex output tex-formatted manual pages

1409 4.1.3 ctp_tools

prog:ctp_tools

1410 Runs charge transport tools

1411 -h [--help] display this help and exit
1412 -v [--verbose] be loud and noisy

```

1413     -t [ --nthreads ] arg (=1) number of threads to create
1414     -o [ --options ] arg calculator options
1415     --man output man-formatted manual pages
1416     --tex output tex-formatted manual pages
1417     -e [ --execute ] arg List of tools separated by ',' or ''
1418     -l [ --list ] Lists all available tools
1419     -d [ --description ] arg Short description of a tool

```

1420 4.1.4 ctp_run

prog:ctp_run

```

1421 Runs charge transport calculators
1422     -h [ --help ] display this help and exit
1423     -v [ --verbose ] be loud and noisy
1424     -o [ --options ] arg calculator options
1425     -f [ --file ] arg sqlight state file, *.sql
1426     -i [ --first-frame ] arg (=1) start from this frame
1427     -n [ --nframes ] arg (=1) number of frames to process
1428     -t [ --nthreads ] arg (=1) number of threads to create
1429     -s [ --save ] arg (=1) whether or not to save changes to state file
1430     -e [ --execute ] arg List of calculators separated by ',' or ''
1431     -l [ --list ] Lists all available calculators
1432     -d [ --description ] arg Short description of a calculator
1433     --man output man-formatted manual pages
1434     --tex output tex-formatted manual pages

```

1435 4.1.5 ctp_parallel

prog:ctp_parallel

```

1436 Runs job-based heavy-duty calculators
1437     -h [ --help ] display this help and exit
1438     -v [ --verbose ] be loud and noisy
1439     -o [ --options ] arg calculator options
1440     -f [ --file ] arg sqlite state file, *.sql
1441     -i [ --first-frame ] arg (=1) start from this frame
1442     -n [ --nframes ] arg (=1) number of frames to process
1443     -t [ --nthreads ] arg (=1) number of threads to create
1444     -s [ --save ] arg (=1) whether or not to save changes to state file
1445     -r [ --restart ] arg restart pattern: 'host(pc1:234) stat(FAILED)'
1446     -c [ --cache ] arg (=8) assigns jobs in blocks of this size
1447     -j [ --jobs ] arg (=run) task(s) to perform: input, run, import
1448     -m [ --maxjobs ] arg (=-1) maximum number of jobs to process (-1 = inf)
1449     -e [ --execute ] arg List of calculators separated by ',' or ''
1450     -l [ --list ] Lists all available calculators
1451     -d [ --description ] arg Short description of a calculator
1452     --man output man-formatted manual pages
1453     --tex output tex-formatted manual pages

```

1454 4.1.6 moo_overlap

prog:moo_overlap

```

1455     -h [ --help ] display this help and exit
1456     -v [ --verbose ] be loud and noisy
1457     --man output man-formatted manual pages
1458     --tex output tex-formatted manual pages
1459     --conjseg arg xml file describing two conjugated segments
1460     --pos1 arg position and orientation of molecule 1

```


1461 --pos2 arg position and orientation of molecule 2
 1462 --pdb arg (=geometry.pdb) pdb file of two molecules

1463 4.2 Calculators

see:calculators

1464 Calculator is a piece of code which computes specific system properties, such as site energies,
 1465 transfer integrals, etc. `ctp_run`, `kmc_run` are wrapper programs which executes such calcula-
 1466 tors. The generic syntax is

1467 `ctp_run -e "calc1, calc2, ..." -o options.xml`

1468 File `options.xml` lists all options needed to run a specific calculator. The format of this file is
 1469 explained in listing 4.1. A complete list of calculators is given in the `calculators` reference section.

list:calc

Listing 4.1: A part of the `options.xml` file with options for the `calculator_name{1,2}` calculators.

```
1470 <calculator_name1>
1471     <option1>value1</option1>
1472     <option2>value2</option2>
1473     ...
1474 </calculator_name1>
1475
1476 <calculator_name2>
1477     <option1>value1</option1>
1478     <option2>value2</option2>
1479     ...
1480 </calculator_name2>
1481 ...
1482
1483
```

1484 A list of all calculators and their short descriptions can be obtain using

1485 `ctp_run --list`

1486 A detailed description of all options of a specific calculator(s) is available via

1487 `ctp_run --desc calc1,calc2,...`

1488 4.2.1 coupling

calc:coupling

1489 Electronic couplings from log and orbital files (GAUSSAIN, TURBOMOLE, NWChem)

option	default	unit	description
package			First-principles package
output	coupling.out.xml		Output file
degeneracy	0	eV	Criterion for the degeneracy of two levels
moleculeA			
log	A.log		Log file of molecule A
orbitals	A.orb		Orbitals file
levels	3		Output HOMO, ..., HOMO-levels; LUMO, ..., LUMO+levels
trim	2		
moleculeB			
log	B.log		Log file of molecule B
orbitals	B.orb		Orbitals file
levels	3		Output HOMO, ..., HOMO-levels; LUMO, ..., LUMO+levels
trim	2		
dimerAB			
log	AB.log		Log file of dimer AB
orbitals	A.orb		Orbitals file

1490 Return to the description of coupling.

1491 4.2.2 log2mps

calc:log2mps
1492

Generates an mps-file (with polar-site definitions) from a QM log-file

option	default	unit	description
package			QM package
logfile			Log-file generated by QM package, with population/esp-fit data

1493 Return to the description of log2mps.

1494 4.2.3 molpol

calc:molpol
1495

Molecular polarizability calculator (and optimizer)

option	default	unit	description
mpsfiles			
input			mps input file
output			mps output file
polar			xml file with infos on polarizability tensor
induction			
expdamp			Thole sharpness parameter
wSOR			mixing factor for convergence
maxiter			maximum number of iterations
tolerance			rel. tolerance for induced moments
target			
optimize			if 'true', refine atomic polarizabilities to match molecular polarizable volume specified in target.molpol
molpol			target polarizability tensor in format xx xy xz yy yz zz (this should be in the eigen-frame, hence xy = xz = yz = 0), if optimize=true the associated polarizable volume will be matched iteratively and the resulting set of polar sites written to mpsfiles.output
tolerance			relative tolerance when optimizing the polarizable volume

1496 Return to the description of molpol.

1497 4.2.4 pdb2map

calc:pdb2map
1498

Converts MD + QM files to VOTCA mapping. Combinations: pdb+xyz,gro+xyz,pdb

option	default	unit	description
pdb	conf.pdb		Input pdb file
gro	conf.gro		Input gro file
xyz	conf.xyz		Input xyz file
xml	conf.xml		Resulting xml file

1499 Return to the description of pdb2map.

1500 4.2.5 pdb2top

calc:pdb2top
1501

Generates fake Gromacs topology file .top

option	default	unit	description
num	1		Num of mols in the box
pdb	conf.pdb		Input pdb file

gro | conf.gro | | Input gro file

1502 Return to the description of `pdb2top`.

1503 4.2.6 `ptopreader`

calc:ptopreader

1504 Reads binary `.ptop`-files (serialized from `ewdbgpol`) and processes them into something readable

option	default	unit	description
<code>ptop_file</code>			Binary archive <code>.ptop</code> -file

1505 Return to the description of `ptopreader`.

1506 4.2.7 `eanalyze`

calc:eanalyze

1507 Histogram and correlation function of site energies and pair energy differences

option	default	unit	description
<code>resolution_sites</code>		eV	Bin size for site energy histogram
<code>resolution_pairs</code>		eV	Bin size for pair energy histogram
<code>resolution_space</code>		eV	Bin size for site energy correlation
<code>states</code>			?

1508 Return to the description of `eanalyze`.

1509 4.2.8 `eimport`

calc:eimport

1510 Imports site energies from the output file of `emultipole` and writes them to the state file

option	default	unit	description
--------	---------	------	-------------

1511 Return to the description of `eimport`.

1512 4.2.9 `einternal`

calc:einternal

1513 Reads in site and reorganization energies and writes them to the state file

option	default	unit	description
<code>energiesXML</code>			XML input file with vacuum site, reorganization (charging, discharging) energies

1514 Return to the description of `einternal`.

1515 4.2.10 `emultipole`

calc:emultipole

1516 Evaluates polarization contribution based on the Thole model

option	default	unit	description
<code>multipoles</code>			Polar Site Definitions in GDMA punch-file format
<code>control</code>			Control options for induction computation
<code>induce</code>	1		Enter '1' / '0' to toggle induction on / off
<code>first</code>			First segment for which to compute site energies
<code>last</code>			Last segment for which to compute site energies
<code>output</code>			File to write site energies to. Site energies are also stored in the state file
<code>check</code>			Check mapping of polar sites to fragment

tholeparam			Thole parameters required for charge-smearing
cutoff		nm	Cut-off beyond which all interactions are neglected
cutoff2		nm	Cut-off beyond which polarization is neglected
expdamp			Damping exponent used in exponential damping function
scaling			1-n interaction scaling, currently not in use
esp			Control options for potential calculation
calcESP			Enter '1' / '0' to toggle on / off. If '1', site energies will not be evaluated
cube			
grid			XYZ file specifying grid points for potential evaluation
output			File to write grid-point potential to
esf			Control options for field calculation
calcESF			Enter '1' / '0' to toggle on / off. If '1', site energies will not be evaluated
grid			XYZ file specifying grid points for field evaluation
output			File to write grid-point field to
alphamol			Control options for molecular-polarizability calculation
calcAlpha			Enter '1' / '0' to toggle on / off. If '1', site energies will not be evaluated
output			File to write polarizability tensor in global frame and in diagonal form to
convparam			Convergence parameters for self-consistent field calculation
wSOR_N			Mixing factor for successive overrelaxation of neutral system, usually between 0.3 and 0.5
wSOR_C			Mixing factor for successive overrelaxation of charged system, usually between 0.3 and 0.5
tolerance			Convergence criterion, fulfilled if relative change smaller than tolerance
maxiter			Maximum number of iterations in the convergence loop

1517 Return to the description of `emultipole`.

1518 4.2.11 `eoutersphere`

calc:eoutersphere

1519 Evaluates outersphere reorganization energy

option	default	unit	description
multipoles			XML allocation polar sites
method			Type of the method: <code>constant</code> - all pairs have value <code>lambda</code> . <code>spheres</code> - molecules are treated as spheres with radii <code>radius</code> and Pekar factor <code>pekar</code> . <code>dielectric</code> - with Pekar factor <code>pekar</code> and partial charges from resulting dielectric fields
lambdaconst		eV	The value for all pairs in the <code>constant</code> method
pekar			Pekar factor used for methods <code>spheres</code> and <code>dielectric</code>
segment			
type			
radius			
segment			
type			
radius			
cutoff		nm	Cutoff radius in between pair and the exterior molecule. Can be used in <code>spheres</code> and <code>dielectric</code>

1520 Return to the description of `eoutersphere`.

1521 **4.2.12 ewdbgpol**

calc:ewdbgpol
1522 Calculates background polarisation needed for ewald calc

option	default	unit	description
multipoles			
control			
mps_table			
pdb_check			
coulombmethod			
method			
cutoff			
shape			
polarmethod			
method			
induce			
cutoff			
convergence			
energy			
kfactor			
rfactor			

1523 Return to the description of ewdbgpol.

1524 **4.2.13 ianalyze**

calc:ianalyze
1525 Evaluates a histogram of a logarithm of squared couplings

option	default	unit	description
resolution_logJ2			Bin size of histogram log(J ²)
states			States for which to calculate the histogram. Example: 1 -1

1526 Return to the description of ianalyze.

1527 **4.2.14 iimport**

calc:iimport
1528 Imports electronic couplings from xml of ctp-dipro using folders of pairdump

option	default	unit	description
idft_jobs_file			idft jobs file

1529 Return to the description of iimport.

1530 **4.2.15 izindo**

calc:izindo
1531 Semiempirical electronic coupling elements for all neighbor list pairs

option	default	unit	description
orbitalsXML			File with paths to .orb files

1532 Return to the description of izindo.

1533 **4.2.16 jobwriter**

calc:jobwriter
1534 Writes list of jobs for a parallel excusion

option	default	unit	description
--------	---------	------	-------------

keys			job type
states	n e h		hole, electron, neutral: mps file is required
single_id			Segment ID as argument for mps.single
kmc_cutoff		nm	Pair-interaction cut-off as argument for mps.kmc

1535 Return to the description of `jobwriter`.

1536 4.2.17 neighborlist

calc:neighborlist

1537 Constructs a list of neighboring conjugated segments

option	default	unit	description
constant	0.5	nm	If provided, this value is used for all segment types
segments			A pair of segment types
type			Types of two segments. For types A and B this can be A A, A B or B B
cutoff		nm	Cutoff radius for centers of mass of rigid fragments

1538 Return to the description of `neighborlist`.

1539 4.2.18 pairdump

calc:pairdump

1540 Coordinates of molecules and pairs from the neighbor list

option	default	unit	description
molecules			If true outputs single molecules, otherwise only pairs

1541 Return to the description of `pairdump`.

1542 4.2.19 profile

calc:profile

1543 Density and site energy profiles

option	default	unit	description
axis			Axis along which to calculate density and energy profiles
direction	0 0 1		Axis direction
min		nm	Minimal projected position for manual binning
max		nm	Maximal projected position for manual binning
bin	0.1	nm	Spatial resolution of the profile
auto	1		'0' for manual binning using min and max, '1' for automated
particles			
type	segments		What centers of mass to use: 'segments' or 'atoms'
first	1		ID of the first segment
last	-1		ID of the last segment, -1 is the list end
output			
density	density.dat		Density profile file
energy	energy.dat		Energy profile file

1544 Return to the description of `profile`.

1545 4.2.20 rates

calc:rates

1546 Hopping rates using classical or semi-classical expression

option	default	unit	description
--------	---------	------	-------------

field			Field in x y z direction
temperature		K	Temperature for rates
method			Method chosen to compute rates. Can either be marcus or jortner . The first is the high temperature limit of Marcus theory, the second is the rate proposed by Jortner and Bixon
nmaxvib	20		If the method of choice is jortner , the maximal number of excited vibrations on the molecules has to be specified as an integer for the summation
omegavib	0.2	eV	If the method of choice is jortner , the vibration frequency of the quantum mode has to be given in units of eV. The default value is close to the CC bond-stretch at 0.2eV

1547 Return to the description of `rates`.

1548 **4.2.21 sandbox**

calc:sandbox

1549 Sandbox to test ctp classes

option	default	unit	description
ID			Not in use

1550 Return to the description of `sandbox`.

1551 **4.2.22 stateserver**

calc:stateserver

1552 Export SQLite file to human readable format

option	default	unit	description
out			Output file name
pdb			PDB coordinate file name
keys			Sections to write to readable format (topology, segments, pairs, coordinates)

1553 Return to the description of `stateserver`.

1554 **4.2.23 tdump**

calc:tdump

1555 Coarse-grained and back-mapped (using rigid fragments) trajectories

option	default	unit	description
md	MD.pdb		Name of the coarse-grained trajectory
qm	QM.pdb		Name of the trajectory with back-substituted rigid fragments
frames	1		Number of frames to output

1556 Return to the description of `tdump`.

1557 **4.2.24 vaverage**

calc:vaverage

1558 Computes site-centered velocity averages from site occupancies

option	default	unit	description
carriers			Carrier types for which to compute velocity averages
tabulate			Tabulate 'atoms' or 'segments'

1559 Return to the description of `vaverage`.

1560 4.2.25 `zmultipole`

1561 `calc:zmultipole`

Evaluates polarization contribution based on the Thole model

option	default	unit	description
<code>multipoles</code>			Polar Site Definitions in GDMA punch-file format
<code>control</code>			Control options for induction computation
<code>induce</code>	1		Enter '1' / '0' to toggle induction on / off
<code>first</code>			First segment for which to compute site energies
<code>last</code>			Last segment for which to compute site energies
<code>output</code>			File to write site energies to. Site energies are also stored in the state file
<code>check</code>			Check mapping of polar sites to fragment
<code>tholeparam</code>			Thole parameters required for charge-smearing
<code>cutoff</code>		nm	Cut-off beyond which all interactions are neglected
<code>cutoff2</code>		nm	Cut-off beyond which polarization is neglected
<code>expdamp</code>			Damping exponent used in exponential damping function
<code>scaling</code>			1-n interaction scaling, currently not in use
<code>esp</code>			Control options for potential calculation
<code>calcESP</code>			Enter '1' / '0' to toggle on / off. If '1', site energies will not be evaluated
<code>cube</code>			
<code>grid</code>			XYZ file specifying grid points for potential evaluation
<code>output</code>			File to write grid-point potential to
<code>esf</code>			Control options for field calculation
<code>calcESF</code>			Enter '1' / '0' to toggle on / off. If '1', site energies will not be evaluated
<code>grid</code>			XYZ file specifying grid points for field evaluation
<code>output</code>			File to write grid-point field to
<code>alphamol</code>			Control options for molecular-polarizability calculation
<code>calcAlpha</code>			Enter '1' / '0' to toggle on / off. If '1', site energies will not be evaluated
<code>output</code>			File to write polarizability tensor in global frame and in diagonal form to
<code>convparam</code>			Convergence parameters for self-consistent field calculation
<code>wSOR_N</code>			Mixing factor for successive overrelaxation of neutral system, usually between 0.3 and 0.5
<code>wSOR_C</code>			Mixing factor for successive overrelaxation of charged system, usually between 0.3 and 0.5
<code>tolerance</code>			Convergence criterion, fulfilled if relative change smaller than tolerance
<code>maxiter</code>			Maximum number of iterations in the convergence loop

1562 Return to the description of `zmultipole`.

1563 4.2.26 `edft`

1564 `calc:edft`

A wrapper for first principles based single site calculations

option	default	unit	description
<code>job</code>			Job options
<code>tasks</code>	input,run,parse		What to run
<code>store</code>	orbitals		What to store

1565 [Return to the description of `edft`.](#)

1566 **4.2.27 idft**

calc:idft

1567 Projection method for electronic couplings. Requires `edft` output

option	default	unit	description
tasks	input,run,parse		What to do
store	orbitals,overlap		What to store
degeneracy	0	eV	Criterion for the degeneracy of two levels
levels	3		Output between HOMO, ..., HOMO-levels; LUMO, ..., LUMO+levels
trim	2		Use trim*occupied of virtual orbitals

1568 [Return to the description of `idft`.](#)

1569 **4.2.28 pewald3d**

calc:pewald3d

1570 Evaluates site energies in a periodic setting

option	default	unit	description
jobcontrol			
job_file			
multipoles			
mapping			
mps_table			
pdb_check			
coulombmethod			
method			
cutoff			
shape			
polarmethod			
method			
induce			
cutoff			
tasks			
calculate_fields			
polarize_fg			
evaluate_energy			
coarsegrain			
cg_background			
cg_foreground			
cg_radius			
cg_anisotropic			
convergence			
energy			
kfactor			
rfactor			

1571 [Return to the description of `pewald3d`.](#)

1572 **4.2.29 qmmm**

calc:qmmm

1573 QM/MM with the Thole MM model

option	default	unit	description
--------	---------	------	-------------

control			
pdb_check			PDB file of polar sites
write_chk	dipoles.xyz		XYZ file with dipoles split onto point charges
format_chk	xyz		format, gaussian or xyz
split_dpl	1		'0' do not split dipoles onto point charges, '1' do split
dpl_spacing	1e-3	nm	Spacing to be used when splitting dipole onto point charges: $d = q * a$
qmpackage			
package			QM package to use for the QM region
gwbse			Specify if GW/BSE excited state calculation ist needed
gwbse_options			GW/BSE options file
state			Number of excited state, which is to be calculated
type			Character of the excited state to be calculated
filter			Filter with which to find the excited state after each calculation
oscillator_strength			Oscillator strength filter, only states with higher oscillator strength are considered
charge_transfer			Charge transfer filter , only states with charge transfer above threshold are considered
qmmmconvg			convergence criteria for the QM/MM
dR	0.001	nm	RMS of coordinates
dQ	0.001	e	RMS of charges
dE_QM	0.0001	eV	Energy change of the QM region
dE_MM	0.0001	eV	Energy change of the MM region
max_iter	10		Number of iterations
coulombmethod			Options for the MM embedding
method	cut-off		Method for evaluation of electrostatics
cutoff1			Cut-off for the polarizable MM1 shell
cutoff2			Cut-off for the static MM2 shell
tholemodel			Parameters for teh Thole model
induce			'1' - induce '0' - no induction
induce_intra_pair			'1' - include mutual interaction of induced dipoles in the QM region. '0' - do not
exp_damp	0.39		Sharpness parameter
scaling			Bond scaling factors
convergence			Convergence parameters for the MM1 (polarizable) region
wSOR_N			Mixing factor for the successive overrelaxation algorithm for a neutral QM region
wSOR_C			Mixing factor for the successive overrelaxation algorithm for a charged QM region
max_iter	512		Maximal number of iterations to converge induced dipoles
tolerance			Maximum RMS change allowed in induced dipoles

1574 Return to the description of qmmm.

1575 4.2.30 xqmultipole

calc:xqmultipole

1576 Electrostatic interaction and induction energy of charged molecular clusters

option	default	unit	description
multipoles			Polar-site mapping definition
control			
job_file			Job file
emp_file			Polar-background definition, allocation of mps-files to segments

pdb_check			Whether or not to output a pdb-file of the mapped polar sites
format_chk			Format for check-file: 'xyz' or 'gaussian'
split_dpl			Split dipoles onto point charges in check-file
dpl_spacing		nm	Spacing between point charges for check-file output
coulombmethod			
method			Currently only cut-off supported
cutoff1		nm	Full-interaction radius cut-off
cutoff2		nm	Radius of electrostatic buffer
tholemodel			
induce			Induce - or not
induce_intra_pair			Induce mutually within the charged cluster
exp_damp			Thole sharpness parameter
scaling			Bond scaling parameters, currently not used
convergence			
wSOR_N			SOR mixing factor for overall neutral clusters
wSOR_C			SOR mixing factor for overall charged clusters
max_iter			Maximum number of iterations
tolerance			Relative tolerance as convergence criterion

1577 Return to the description of `xqmultiple`.

1578 4.2.31 energy2xml

calc:energy2xml

1579 Write out energies from SQL file

option	default	unit	description
--------	---------	------	-------------

1580 Return to the description of `energy2xml`.

1581 4.2.32 integrals2xml

calc:integrals2xml

1582 Write out transfer integrals from SQL file

option	default	unit	description
--------	---------	------	-------------

1583 Return to the description of `integrals2xml`.

1584 4.2.33 occupations2xml

calc:occupations2xml

1585 Write out site occupation probabilities from SQL file

option	default	unit	description
--------	---------	------	-------------

1586 Return to the description of `occupations2xml`.

1587 4.2.34 pairs2xml

calc:pairs2xml

1588 Write out neighbourlist from SQL file

option	default	unit	description
--------	---------	------	-------------

1589 Return to the description of `pairs2xml`.

1590 4.2.35 rates2xml

calc:rates2xml

1591 Write out charge transfer rates from SQL file

option	default	unit	description
--------	---------	------	-------------

1592 Return to the description of rates2xml.

1593 4.2.36 segments2xml

calc:segments2xml

1594 Write out segment data from SQL file

option	default	unit	description
--------	---------	------	-------------

1595 Return to the description of segments2xml.

1596 4.2.37 trajectory2pdb

calc:trajectory2pdb

1597 Generate PDB files for the mapped MD/QM topology

option	default	unit	description
--------	---------	------	-------------

1598 Return to the description of trajectory2pdb.

Bibliography

- poelking_long-range_2016 [1] C. Poelking and D. Andrienko, *Journal of Chemical Theory and Computation* **12**, 4516 (2016). [ii](#), [14](#)
- kordt_modeling_2016 [2] P. Kordt and D. Andrienko, *J. Chem. Theory Comput.* **12**, 36 (2016). [ii](#)
- ruhle_microscopic_2011 [3] V. Rühle *et al.*, *Journal of Chemical Theory and Computation* **7**, 3335 (2011). [ii](#), [3](#), [24](#)
- lukyanov_extracting_2010 [4] A. Lukyanov and D. Andrienko, *Physical Review B* **82**, 193202 (2010). [ii](#), [26](#)
- baumeier_density-functional_2010 [5] B. Baumeier, J. Kirkpatrick, and D. Andrienko, *Physical Chemistry Chemical Physics* **12**, 11103 (2010). [ii](#), [19](#), [21](#), [24](#), [28](#)
- ruhle_versatile_2009 [6] V. Rühle *et al.*, *Journal of Chemical Theory and Computation* **5**, 3211 (2009). [ii](#), [3](#), [6](#)
- kirkpatrick_approximate_2008 [7] J. Kirkpatrick, *International Journal of Quantum Chemistry* **108**, 51 (2008). [ii](#), [23](#)
- gamma_design_1995 [8] E. Gamma, R. Helm, and R. E. Johnson, *Design Patterns. Elements of Reusable Object-Oriented Software.*, 1st ed., reprint. ed. (Addison-Wesley Longman, Amsterdam, ADDRESS, 1995). [3](#)
- ruhle_multiscale_2010 [9] V. Rühle, J. Kirkpatrick, and D. Andrienko, *The Journal of Chemical Physics* **132**, 134103 (2010). [7](#)
- vukmirovic_charge_2008 [10] N. Vukmirović and L.-W. Wang, *The Journal of Chemical Physics* **128**, 121102 (2008). [7](#)
- vukmirovic_charge_2009 [11] N. Vukmirović and L.-W. Wang, *Nano Letters* **9**, 3996 (2009).
- mcmahon_ad_2009 [12] D. P. McMahon and A. Troisi, *Chemical Physics Letters* **480**, 210 (2009). [7](#)
- bredas_charge-transfer_2004 [13] J.-L. Brédas, D. Beljonne, V. Coropceanu, and J. Cornil, *Chemical Reviews* **104**, 4971 (2004). [8](#), [24](#)
- may_charge_2011 [14] V. May and O. Kühn, *Charge and Energy Transfer Dynamics in Molecular Systems*, 3rd, revised and enlarged edition ed. (Wiley-VCH, Weinheim, 2011). [9](#), [25](#)
- breneman_determining_1990 [15] C. M. Breneman and K. B. Wiberg, *Journal of Computational Chemistry* **11**, 361 (1990). [11](#)
- stone_distributed_1985 [16] A. Stone and M. Alderton, *Molecular Physics* **56**, 1047 (1985). [11](#), [12](#)
- chirlian_atomic_1987 [17] L. E. Chirlian and M. M. Francl, *Journal of Computational Chemistry* **8**, 894 (1987). [11](#)
- singh_approach_1984 [18] U. C. Singh and P. A. Kollman, *Journal of Computational Chemistry* **5**, 129 (1984). [11](#)
- stone_distributed_2005 [19] A. J. Stone, *Journal of Chemical Theory and Computation* **1**, 1128 (2005). [12](#)
- stone_theory_1997 [20] A. J. Stone, *The Theory of intermolecular forces* (Clarendon Press, Oxford, 1997). [13](#)
- thole_molecular_1981 [21] B. T. Thole, *Chemical Physics* **59**, 341 (1981). [13](#)
- van_duijnen_molecular_1998 [22] P. T. van Duijnen and M. Swart, *The Journal of Physical Chemistry A* **102**, 2399 (1998). [13](#), [14](#)
- applequist_atom_1972 [23] J. Applequist, J. R. Carl, and K.-K. Fung, *Journal of the American Chemical Society* **94**, 2952 (1972). [13](#)
- ren_polarizable_2003 [24] P. Ren and J. W. Ponder, *The Journal of Physical Chemistry B* **107**, 5933 (2003). [13](#), [14](#)
- baessler_charge_1993 [25] H. Baessler, *Physica Status Solidi B* **175**, 15 (1993). [19](#), [24](#)
- troisi_charge-transport_2006 [26] A. Troisi and G. Orlandi, *Physical Review Letters* **96**, 086601 (2006).
- troisi_charge_2009 [27] A. Troisi, D. L. Cheung, and D. Andrienko, *Physical Review Letters* **102**, 116602 (2009).
- mcmahon_organic_2010 [28] D. P. McMahon and A. Troisi, *ChemPhysChem* **11**, 2067 (2010).

- [vehoff_charge_2010](#) [29] T. Vehoff, B. Baumeier, A. Troisi, and D. Andrienko, *Journal of the American Chemical Society* **132**, 11702 (2010). 19
- [walker_electrical_2002](#) [30] A. B. Walker, A. Kambili, and S. J. Martin, *Journal of Physics: Condensed Matter* **14**, 9825 (2002). 24
- [borsenberger_charge_1991](#) [31] P. M. Borsenberger, L. Pautmeier, and H. Bässler, *The Journal of Chemical Physics* **94**, 5447 (1991).
- [pasveer_unified_2005](#) [32] W. F. Pasveer *et al.*, *Physical Review Letters* **94**, 206601 (2005). 24
- [bredas_molecular_2009](#) [33] J.-L. Brédas, J. E. Norton, J. Cornil, and V. Coropceanu, *Accounts of Chemical Research* **42**, 1691 (2009). 24
- [coropceanu_charge_2007](#) [34] V. Coropceanu *et al.*, *Chemical Reviews* **107**, 926 (2007).
- [nelson_modeling_2009](#) [35] J. Nelson, J. J. Kwiatkowski, J. Kirkpatrick, and J. M. Frost, *Accounts of Chemical Research* **42**, 1768 (2009). 24
- [marcus_electron_1993](#) [36] R. A. Marcus, *Reviews of Modern Physics* **65**, 599 (1993). 24
- [hutchison_hopping_2005](#) [37] G. R. Hutchison, M. A. Ratner, and T. J. Marks, *Journal of the American Chemical Society* **127**, 2339 (2005). 24
- [chang_new_2005](#) [38] J.-L. Chang, *Journal of Molecular Spectroscopy* **232**, 102 (2005). 24
- [hoffman_reorganization_1996](#) [39] B. M. Hoffman and M. A. Ratner, *Inorganica Chimica Acta* **243**, 233 (1996). 25
- [bortz_new_1975](#) [40] A. B. Bortz, M. H. Kalos, and J. L. Lebowitz, *Journal of Computational Physics* **17**, 10 (1975). 25
- [scher_anomalous_1975](#) [41] H. Scher and E. Montroll, *Physical Review B* **12**, 2455 (1975). 26
- [borsenberger_role_1993](#) [42] P. M. Borsenberger, E. H. Magin, M. D. VanAuweraer, and F. C. D. Schryver, *Physica Status Solidi A* **140**, 9 (1993). 26
- [derrida_velocity_1983](#) [43] B. Derrida, *Journal of Statistical Physics* **31**, 433 (1983). 26, 28
- [cordes_one-dimensional_2001](#) [44] H. Cordes *et al.*, *Physical Review B* **63**, 094201 (2001).
- [seki_electric_2001](#) [45] K. Seki and M. Tachiya, *Physical Review B* **65**, 014305 (2001). 26
- [van_der_holst_modeling_2009](#) [46] J. J. M. van der Holst *et al.*, *Physical Review B* **79**, 085203 (2009). 27
- [dunlap_charge-dipole_1996](#) [47] D. Dunlap, P. Parris, and V. Kenkre, *Physical Review Letters* **77**, 542 (1996). 28
- [novikov_essential_1998](#) [48] S. V. Novikov *et al.*, *Physical Review Letters* **81**, 4472 (1998). 28
- [nagata_atomistic_2008](#) [49] Y. Nagata and C. Lennartz, *The Journal of Chemical Physics* **129**, 034709 (2008). 28
- [novikov_cluster_1995](#) [50] S. V. Novikov and A. V. Vannikov, *The Journal of Physical Chemistry* **99**, 14573 (1995). 28